ANEMI_Yangtze v1.0: A Coupled Human-Natural Systems Model for the Yangtze Economic Belt - Model Description

Haiyan Jiang[1,2,3*], Slobodan P. Simonovic[1], Zhongbo Yu[3,4,5]

[1]Department of Civil and Environmental Engineering, Western University, London, Ontario, Canada

[2]College of Urban Construction, Nanjing Tech University, Nanjing, 211816, China

[3]State Key Laboratory of Hydrology-Water Resources and Hydraulic Engineering, Hohai University, Nanjing, 210098, China[4]Joint International Research Laboratory of Global Change and Water Cycle, Hohai University, Nanjing, 210098, China

[5]Yangtze Institute for Conservation and Development, Hohai University, Nanjing, 210098, China

Correspondence: Haiyan Jiang (sophia4637@163.com; hjiang95@uwo.ca)

Abstract: Yangtze Economic Belt (hereafter Belt) is one of the most dynamic regions in China in terms of population growth, economic progress, industrialization, and urbanization. It faces many resource constraints (land, food, energy) and environmental challenges (pollution, biodiversity loss) under rapid population growth and economic development. Interactions between human and natural systems are at the heart of the challenges facing the sustainable development of the Belt. By adopting the system thinking and the methodology of system dynamics simulation, an integrated system dynamics-based simulation model for the Belt, named ANEMI_Yangtze, is developed based on the third version of ANEMI3. Nine sectors of population, economy, land, food, energy, water, carbon, nutrients, and fish are currently included in ANEMI_Yangtze.

This paper presents the ANEMI_Yangtze model description, which includes: (i) the identification of the cross-sectoral interactions and feedbacks involved in shaping the Belt's system behaviour over time; (ii) the identification of the feedbacks within each sector that drive the state variables in that sector; and (iii) the description of a new *Fish Sector* and modifications in the *Population*, *Food*, *Energy*, and *Water Sectors*, including the underlying theoretical basis for model equations. The validation and robustness tests confirm that the ANEMI_Yangtze model can be used to support scenario development, policy assessment, and decision making. This study aims to improve the understanding of the complex interactions among coupled human-natural systems in the Belt to provide the foundation for science-based policies for the sustainable development of the Belt.

Keywords: ANEMI_Yangtze; coupled human and nature systems; system dynamics simulation; Yangtze Economic Belt

1. Introduction

Today global problems and challenges facing humanity are becoming more and more complex and directly related to the areas of energy, water, and food production, distribution, and use (Hopwood et al., 2005; Bazilian et al., 2011; Akhtar et al., 2013; van Vuuren et al., 2015; D'Odorico et al., 2018). The relations linking human race to the biosphere are so complex that all aspects affect each other. Knowledge and methods from a single discipline are no longer sufficient to address these complex, interrelated problems that characterize as fundamental threats to human society (Klein et al., 2001; Bazilian et al., 2011; Calvin and Bond-Lamberty, 2018; Clayton and Radcliffe, 2018). Understanding the mechanism of the dynamics within the coupled human-natural systems calls for cooperation across wide-range of disciplines and knowledge domains (Liu et al., 2007; Fu, 2020). The combination of quantitative multi-sector modelling and scenario analysis has emerged as a well-suited methodology paradigm for studying coupled human-natural systems and exploring future pathways and policy implications (Hertwich et al., 2015; Allen et al., 2016; Fu, 2020).

Multi-sector modelling mainly occurs within two modelling paradigms: Integrated Assessment Modelling (IAM) and System Dynamics simulation (SD). IAMs are developed and used for addressing complex interactions between socio-economic and natural sectors. They integrate knowledge from various disciplines into a single modelling environment and are used to investigate future adaptation pathways to globally changing conditions (van Beek et al., 2020). There are several IAMs of global change. Examples include AIM (Matsuoka et al., 1995), MESSAGE (Messner and Strubegger, 1995; Messner and Schrattenholzer, 2000; Sullivan et al., 2013), POLES (European Commission, 1996), TIMES (Loulou, 2007), REMIND (Bauer et al., 2012; Kriegler et al., 2017), IMAGE (Stehfest et al., 2014), and GCAM (Calvin et al., 2019), to name a few. The second modelling paradigm - System Dynamics simulation (SD) - integrates all sectoral models into the endogenous structures with emphasis on the link between the system structure and dynamic behaviour through explicit consideration of multiple feedback relations (Davies and Simonovic, 2010; Pedercini et al., 2019; Qu et al., 2020). There are also several SD models of global change. Examples include ANEMI (Davies and Simonovic, 2010, 2011; Akhtar et al., 2013, 2019; Breach and Simonovic, 2021), Threshold 21 (Qu et al., 1995, 2020), and iSDG

(Pedercini et al., 2019). ANEMI is intended for analyzing long-term (2100) global feedbacks with emphasis on the role of water resources. Threshold 21 and iSDG are structured to analyze medium (2030) to long-term (2050) development issues at the national scale.

Both IAMs and SD models provide valuable tools to assess the impacts of global change and adaptation and vulnerability of human society. However, most of these models are highly aggregated. This level of aggregation limits the level of detail that can be represented (Breach and Simonovic, 2021). Therefore, there is an urgent need for model downscaling (Holman et al., 2008; Bazilian et al., 2011; Akhtar et al., 2019; Fisher-Vanden and Weyant, 2020). For example, the GCAM model currently has several sub-national versions, including GCAM-USA (Shi et al., 2017), GCAM-China (Yu et al., 2020), GCAM-Korea (Jeon et al., 2020) and others in development. Recently, there have even been calls for downscaling models to the city level (Dermody et al., 2018). Another way of capturing regional or local processes is to develop regional or local integrated models from scratch. For instance, the coupled water supply-power generation-environment systems model developed for the upper Yangtze river basin in China (Jia et al., 2021). However, due to the considerable complexities in the coupled human-natural systems at the local scale, research aimed at addressing local-specific challenges is still limited, especially for regions with fast socio-economic development (Wang et al., 2019).

Yangtze Economic Belt, one of the most dynamic regions in China in terms of population growth and economic development, accounts for about 40% of the country's population and GDP and 1/15 of the global population. The Belt's fast urbanization and economic prosperity come at the cost of the environment (Xu et al., 2018). To repair its deteriorating eco-environment, the Belt's development paradigm has shifted from "large-scale development" to "green development". However, it remains poorly understood how the coupled human-natural systems in the Belt interact? To enhance understanding of the complex interactions among human and natural systems in the Belt and to provide the foundation for science-based policy-making for the sustainable development of the Belt, we developed the ANEMI_Yangtze model. This paper focuses on model description and would be an important addition to the literature. The model application, which helps us understand how the Belt will evolve under a particular set of conditions and how the system will change in response to a wide range of policy scenarios, is available in Jiang et al. (2021). The rest of the paper is organized as follows: section 2 describes the Belt and its challenges; section 3 illustrates the theoretical basis for ANEMI_Yangtze; new aspects of the model development are provided in section 4; section 5 discusses the model validation and application; and section 6 offers the final conclusions.

2. Yangtze Economic Belt: system description

Yangtze river originates from the Tanggula Mountains on the Plateau of Tibet and flows eastward to the East China Sea. It has a total length of 6,300 km with a catchment area of about 1.8 million km^2. Located mainly in the Yangtze river basin, the Belt traverses eastern, central and western China, joining the coast with the inland and consists of 3 economic zones – the Chongqing-Sichuan upstream urban agglomeration, the central triangle urban agglomeration, and the Yangtze river delta agglomeration, The relationship between the Yangtze river basin and the Belt is shown in Figure 1.

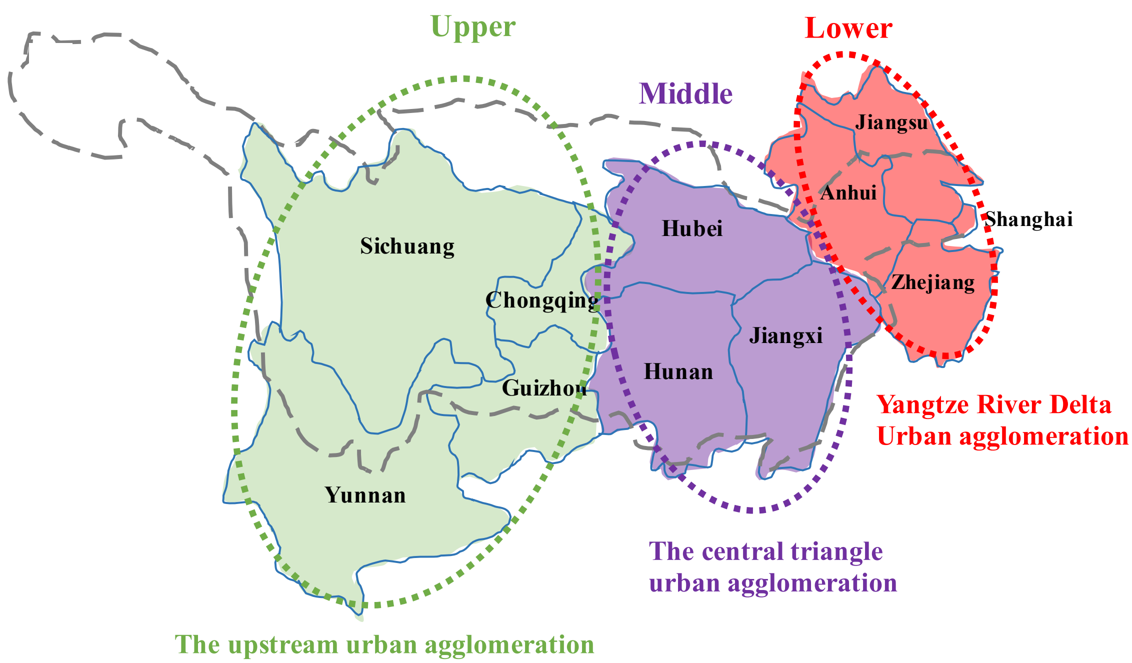

Figure 1. Yangtze river basin (black long dashed line) and the Yangtze Economic Belt

Over the past decades, especially after the reform and opening-up of China in the late 1970s, the Belt has developed into one of the most vital regions in China. It accounts for 21% of the country's total land area (2.05 million km^2) and is home to 40% of the country's total population, with an economic output exceeding 40% of the country's total GDP. The Belt is home to many advanced manufacturing industries, modern service industries, major national infrastructure projects, and high-tech industrial parks. As one of China's most important industrial corridors, the Belt's output of steel, automobile, and petrochemical industries accounts for more than 36%, 47%, and 50% of the total national output, respectively (MIIT, 2016). In 2018, the Belt's population and

GDP were about 599 million and 40.3 trillion RMB, accounting for 42.9% and 44.1% of the country, respectively. As the initiation of the Belt in 2016 and the gradual loosening of China's birth control policy, the Belt's processes of urbanization and industrialization are expected to gain momentum in the coming decades (NDRC, 2016). The fast urbanization and strong economic growth in the Belt, however, pose severe challenges for its sustainable development. These challenges mainly include the climate change impacts, energy crisis, land availability and food security, water pollution, and depletion of fish stock in the river.

2.1 Climate change impacts

The Yangtze river basin is vulnerable to global warming. Accumulating evidence shows that climate change affects the hydrologic regime in the river basin. For example, research finds that the glaciers in the Qinghai-Xizang Plateau in the head Yangtze regions shrank by 7% (3,790 km^2) over the past four decades (Li et al., 2010). Changes in hydrological cycle result in more frequent extreme meteorological events happening in the Yangtze rive basin (Cao et al., 2011; Gu et al., 2015; Su et al., 2017), exposing vast majority of the population to growing physical and socio-economic risks. For example, during the summer of 2020, eight provinces in the Yangtze river basin experienced severe floods, leaving hundreds dead and disrupting the economy's post-pandemic recovery.

2.2 Energy crisis

The Yangtze river basin is poor in fossil fuel endowments even though China's has the world's largest coal reserves. Data from China Energy Statistical Yearbook indicates that in 2015 the Belt imported about 60% of its coal consumption (DENBS, 2016). The Yangtze river basin has, however, abundant hydropower resources. The estimated hydopower potential in the river basin is about 278 million kilowatts (Wang, 2015). The Yangtze coastal areas are ideal locations for nuclear plants. However, due to technical limitations and development costs, coal still dominates energy consumption, accounting for about 56% of total energy consumption currently (Su, 2019).

2.3 Land availability and food security

Statistics from the Demographic Yearbook indicate that the Yangtze river basin's population grew from 500 million in 1990 to about 600 million in 2020, and is expected to reach its peak around 2030 if the one-child policy remains unchanged (Zeng and Hesketh, 2016). As the country's birth control policy gradually loosens, the population in the Belt will grow even faster.

With a high population growth rate and rising income, the consumption of food, especially non-starchy food such as dairy and meat, is expected to increase (Niva et al., 2020). This higher food production has to come from the same amount of land or even less land due to the competing use of land for urbanization. Population growth and urban expansion occupy many rich farmlands. Research shows that from 2000 to 2015 urban areas in the Yangtze river basin increased by 67.51% whereas cropland decreased by 7.53% (Kong et al., 2018).

2.4 Water pollution

The increasing application of fertilizers and pesticides in agriculture and discharging of wastewater from a growing population and rapid industry development lead to severe problems concerning pollution of freshwater, eutrophication of lakes, and deterioration of the water ecosystem. Statistical data indicate that 86.9% of major lakes and 35.1% of major reservoirs in the Yangtze river basin suffer from eutrophication (YRWRC, 2016). Among them, the most serious case is the eutrophication of Lake Taihu, which is located in the floodplain of the lower Yangtze river (Li et al., 2011). In 2007, the blue algal bloom outbreak in Lake Taihu cut off drinking water supply for 2 million citizens in Wuxi city for a whole week (Qin et al., 2007). The last decade has witnessed some 70 million RMB flowing into the eutrophication control of Lake Taihu annualy.

2.5 Depletion of Yangtze fish stock

Fishery resources in the Yangtze river are seriously depleted. To date, wild capture fisheries production decreased to less than 100 thousand tonnes, falling well short of the maximum output of 427 thousand tonnes in the 1950s (Zhang et al., 2020). The eggs and larvae of the four major Chinese carps were approximately 1.11 billion in 2015, accounting for only 1% of historical production in 1965 (Yi et al., 1988; Zhang et al., 2017). Habitat fragmentation and shrinkage as a result of reclamation of lakes for farmland and dam construction, together with overfishing and water pollution, are the main factors threatening aquatic biodiversity in the Yangtze river (Jiang et al., 2020; Zhang et al., 2020). In an effort to protect Yangtze's aquatic life, a 10-year commercial fishing ban was introduced in 2020. Fishing in the main stream of Yangtze river, the Poyang-Dongting lakes, and the seven major tributaries is temporarily banned for a period of 10 years starting from 2021.

3. ANEMI_Yangtze: background and theoretical basis

The ANEMI_Yangtze model currently consists of nine sectors: *Population*, *Economy*, *Land*, *Food*, *Energy*, *Water*, *Carbon*, *Nutrients*, and *Fish*. It is developed based on the ANEMI3 global model (Breach and Simonovic, 2021). The time horizon of the model is 2100 and the simulation step is one year. By introducing a subscript variable, *location* (consists of upper, middle, and lower Belt), we are able to build "one" model to account for the spatial heterogeneity within the Belt's 3 economic zones – the upper Chongqing-Sichuan upstream urban agglomeration, the middle central triangle urban agglomeration, and the lower Yangtze river delta agglomeration. The model is grounded in systems thinking and developed using the system dynamics simulation approach. System dynamics research originated in control engineering and is a valuable methodology for capturing the nonlinearity, feedbacks, and delays in determining the dynamic behaviour of complex systems (Forrester, 1961). In system dynamics, interactions and feedbacks between system components illustrated using Causal Loop Diagram (CLD), are far more important for understanding system behaviour than focusing on separate details (Simonovic, 2009).

3.1 Cross-sectoral interactions and feedbacks

The cross-sectoral interactions and feedback in ANEMI_Yangtze (Figure 2) are discussed in the following section. Capitalized italics are used for sector names and italics are used for names of state variables.

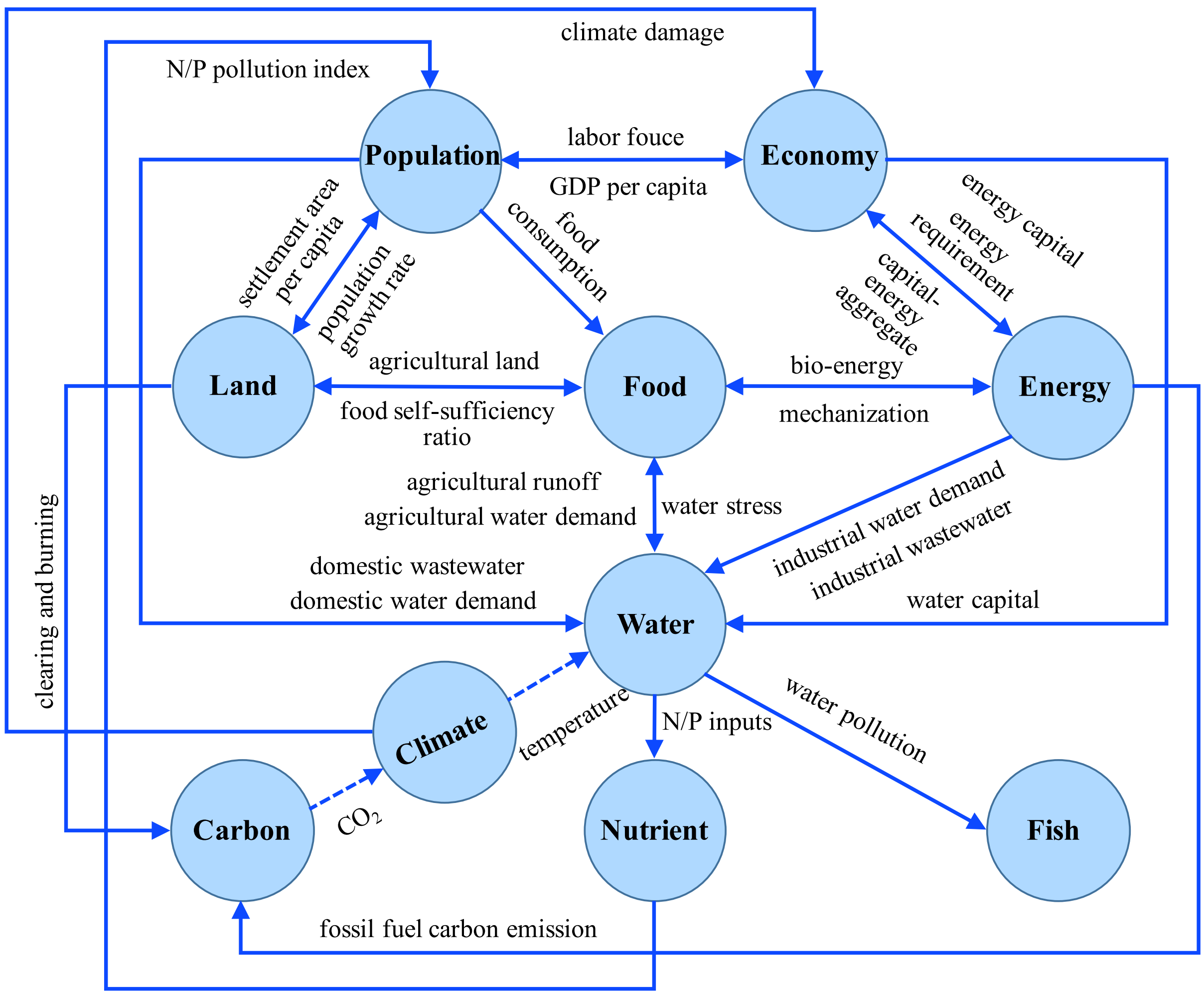

Figure 2. Cross-sectoral interactions among the human-natural systems in the Belt

The *Population and Economy Sectors* are linked through *GDP per capita* and *labour force*. *Population Sector* affects *Economy Sector* through *labour force*, an important element of the Cobb-Douglas production function. *Economy Sector* affects *Population Sector* both positively and negatively through *GDP per capita*. The reasoning behind this impact is that: increased *economic output,* on one hand results in higher quality health services and *life expectancy*, thereby reducing *mortality* rates; on the other hand, high housing price accompanied with economic development usually restrains fertility choices, thus reducing birth rates (Meadows et al., 1974; Dettling and Kearney, 2014; Breach, 2020). In China, the *total fertility* in more developed south-east regions is generally lower than in less developed western regions (Hui et al., 2012; Clark et al., 2020). Economic factor is the most important driver of migration (Lee,1966). The differences in *GDP per capita* among the Belt's three economic zones affect population migration within the Belt.

The *Population*, *Food*, and *Land Sector*s are connected through *population growth rate*, *food self-sufficiency ratio*, and *settlement area per capita*. Population growth accelerates the transfer rate of biome among different land-use types (Goudriaan and Ketner, 1984). Population growth drives *food consumption*, thereby decreasing *food self-sufficiency*, resulting in more agricultural land being converted by clearing and burning forests and grassland. Population growth also leads to more agricultural land around the urban area be claimed for settlement use as urban expands. The *Land Sector* negatively impacts population growth as increased population places more stress on *settlement area per capita*, which then acts as an opposing force on the migration rate (this feedback is further clarified in section 4.3).

The *Economy* and *Energy Sector*s are linked through *capital-energy aggregate*, *energy capital*, and *energy requirement*. A growing economy increases the need for energy, which drives *energy production* through increasing *energy capital* investment. An increase in *energy capital* further intensifies the *capital-energy aggregate*, driving economy growth, thus forming a positive feedback loop.

The *Population*, *Food*, *Energy*, and *Water Sector*s are connected via *domestic water demand* and *consumption*, *agricultural water demand* and *consumption*, and *industrial water demand* and *consumption*. Water plays a vital role in food production and is needed in almost every stage of energy extraction, production, processing, and especially consumption. With increased population and demand for food and energy, the total demand for and consumption of water increases, increasing *water stress*, which in turn, impedes population growth and *food production* (Dinar et al., 2019; Breach, 2020). The increasing *water stress* also drives more capital flowing into water supply development so as to alleviate *water stress*, thus connecting the *Economy* sector with the *Water Sector*.

The use of water by *Population*, *Energy*, and *Food Sector*s all results in water pollution in the form of increased nutrient concentration through the discharge of *domestic* and *industrial wastewater* and *agricultural runoff*. This links *Water Sector* with *Nutrient Sector*. An increased level of *nutrient concentration* negatively affects population growth through *life expectancy multiplier* (Pautrel, 2009), thus links the *Nutrient-Population Sectors*. Water pollution also endangers fish by increasing the population's *natural mortality rate* (Zhang et al., 2020).

The *Carbon* and *Land Sector*s are connected through clearing and burning, while the *Carbon* and *Energy Sector*s are connected through *fossil fuel emissions*. The *Carbon-Climate* sector feedback depends on the atmospheric CO_2 concentration determined by the *Carbon* sector. The climate change effect is treated exogenously. The *Climate* and *Water Sector*s are connected via the *surface temperature change*. Since increased surface temperature will likely increase the intensity of hydrological cycle (Giorgi et al., 2011), the model includes a temperature multiplier equation that increases evaporation and evapotranspiration. The *Climate Sector* influences the *Economy* sector through a temperature damage function, developed by Nordhaus and Boyer (2000).

3.2 Interactions and feedbacks within model sectors

3.2.1 CLD in *Population Sector*

The three variables - *births, deaths,* and *migrants*, which are all affected by *GDP per capita*, drive the dynamic behaviour of the populatio*n* in the Belt. *GDP per capita*, which is affected by *labour force* and *gross output*, rises if the effect of the increase in the *gross output* outpaces the effect of the population increase, and vice versa. So, any loops containing *GDP per capita* can either be positive or negative depending on whether it is increasing or decreasing with population growth. Figure 3 shows the feedbacks in *Population Sector*. The positive loop A1 and negative loop B1 depict the effect of *GDP per capita* on mortality, whereas positive loop C1 and negative loop D1 on fertility. The positive loop E1 and negative loop F1 illustrate the impact of *GDP difference factor* on migration, whereas loop G1 explains the effect of crowding on migration. The process of and mechanism behind the CLD are illustrated in sections 3.1 and 4.3.

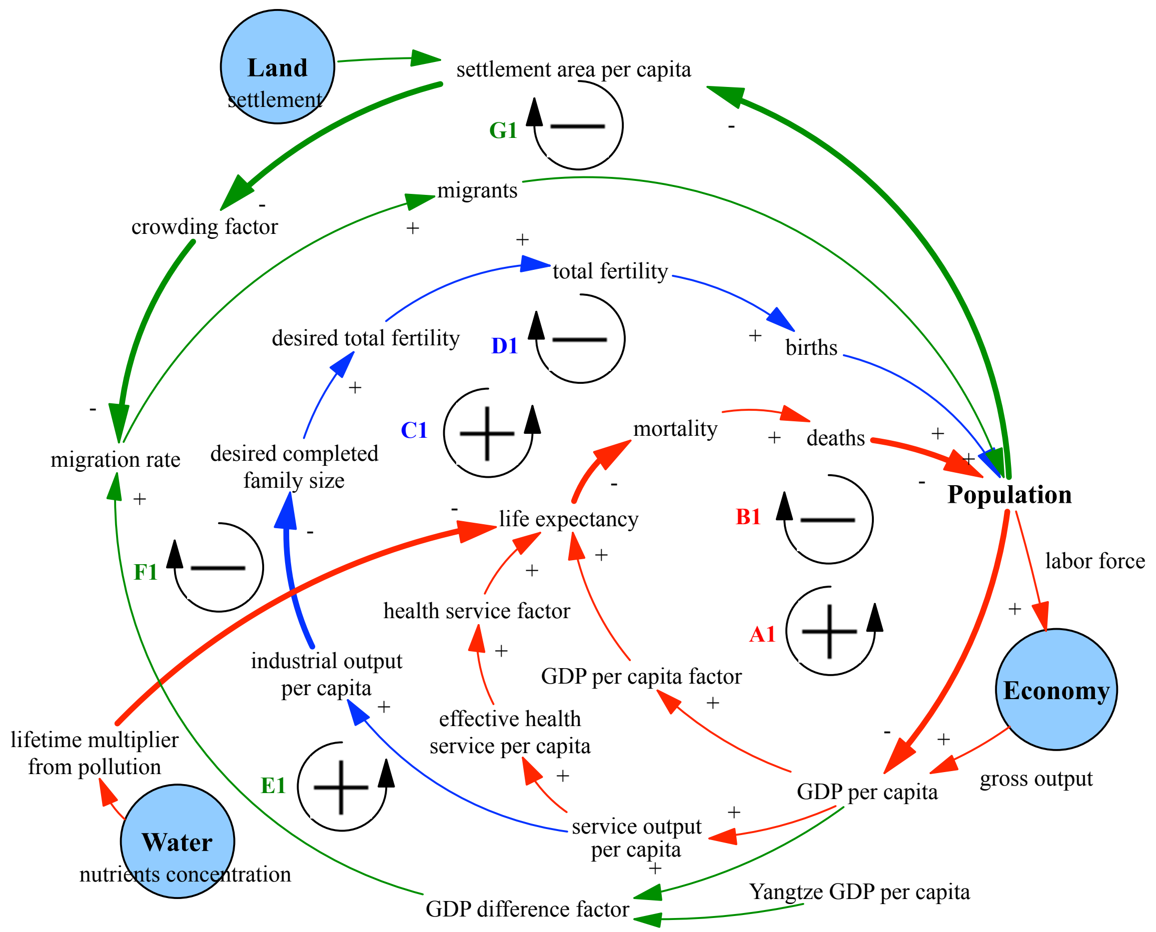

Figure 3. CLD in *Population Sector*

3.2.2 CLD in *Economy Sector*

Figure 4 displays the interactions and feedbacks in *Economy Sector*. Capital orders respond to three pressures. Orders first replace depreciation (loops D2 and E2). Loop E2 depicts the process of depreciation, which slowly depletes *capital* stock. Loop D2 compensates for depreciation by factoring it into *desired capital order rate*. Orders then correct the gap between desired and actual capital (loop C2). *Desired capital* stock is anchored on real *capital* stock and adjusted for relative cost and *marginal product of capital* (loops A2 and B2). Finally, orders augment *capital* stock in order to anticipate output growth. See also Fiddaman (1997) and Breach (2020) for detailed process of and mechanism behind the CLD in *Economy Sector*.

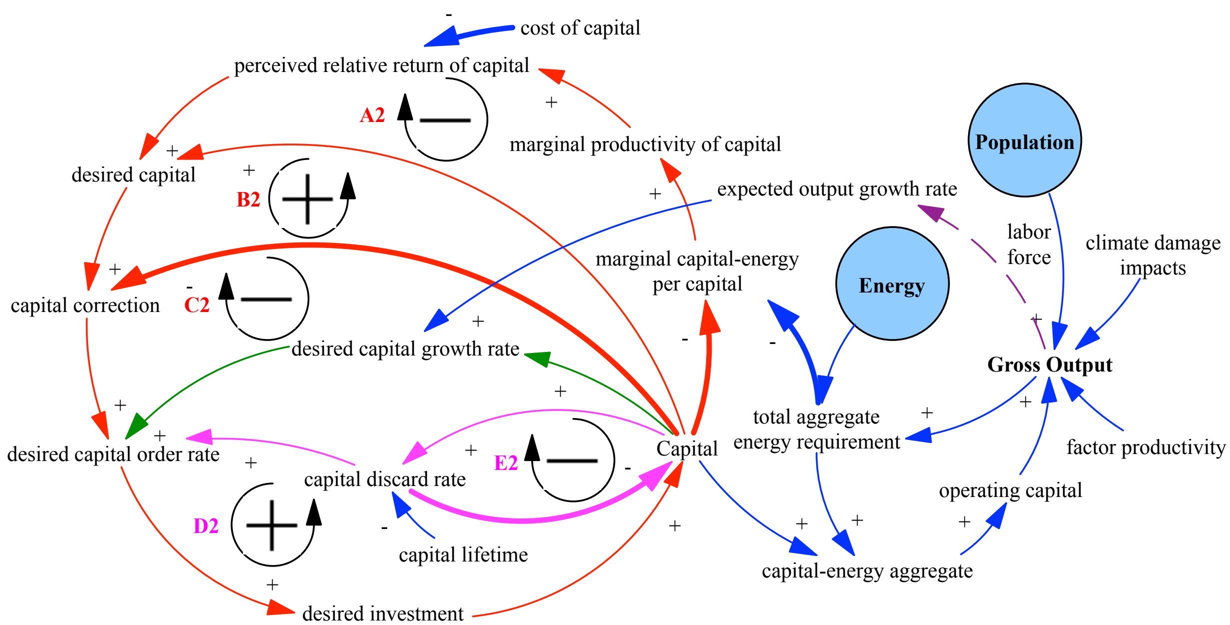

Figure 4. CLD in *Economy Sector*

3.2.3 CLD in *Land Sector*

Figure 5 illustrates the feedbacks in *agricultural land* (the feedback in the *forest*, *grassland*, *wetland*, *settlement*, and *other land*, which are not shown in the figure, are the same as those in the *agricultural land*). An increase in the stock of *agricultural land* increases its transfer rate to the *forest*, *grassland*, *wetland*, *settlement*, and *other land*, which all together drain the stock of *agricultural land* and form the negative loops A3, B3, C3, D3, and E3.

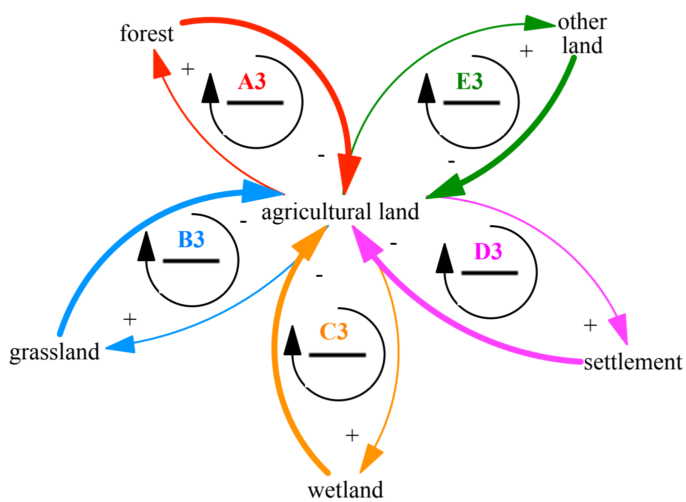

Figure 5. CLD in *agricultural land*

3.2.4 CLD in *Food Sector*

Figure 6 shows the CLD in *Food Sector*. Negative loops A4, B4, and C4 illustrate the impacts of *land yield technology*, *agricultural land development*, and *fertilizer subsidy*, respectively, on *food production* through the indicator of *food self-sufficiency ratio*. A decrease in *food self-sufficiency ratio* stimulates inputs in *land yield technology*, *agricultural land development*, and *fertilizer subsidy*, which all drive up *land yield*, resulting in increases in *food production* and *food self-sufficiency ratio* (Ju et al., 2020). Changes in agricultural product prices are recognized as significant factors driving grain production (Xie and Wang, 2017). Negative loops E4 and F4 depict the introduction of multiple cropping practices (*multiple cropping index*) and *willingness to increase grain planting area* on *food production* through *food price change*. An increase in *food price change* acts as positive feedback on farmers' adopting of multiple cropping practices (*multiple cropping index*) and increasing *grain planting area*. Positive loop D4 counterbalances the effect of adopting multiple cropping practices by decreasing *land fertility* and the corresponding *land yield*.

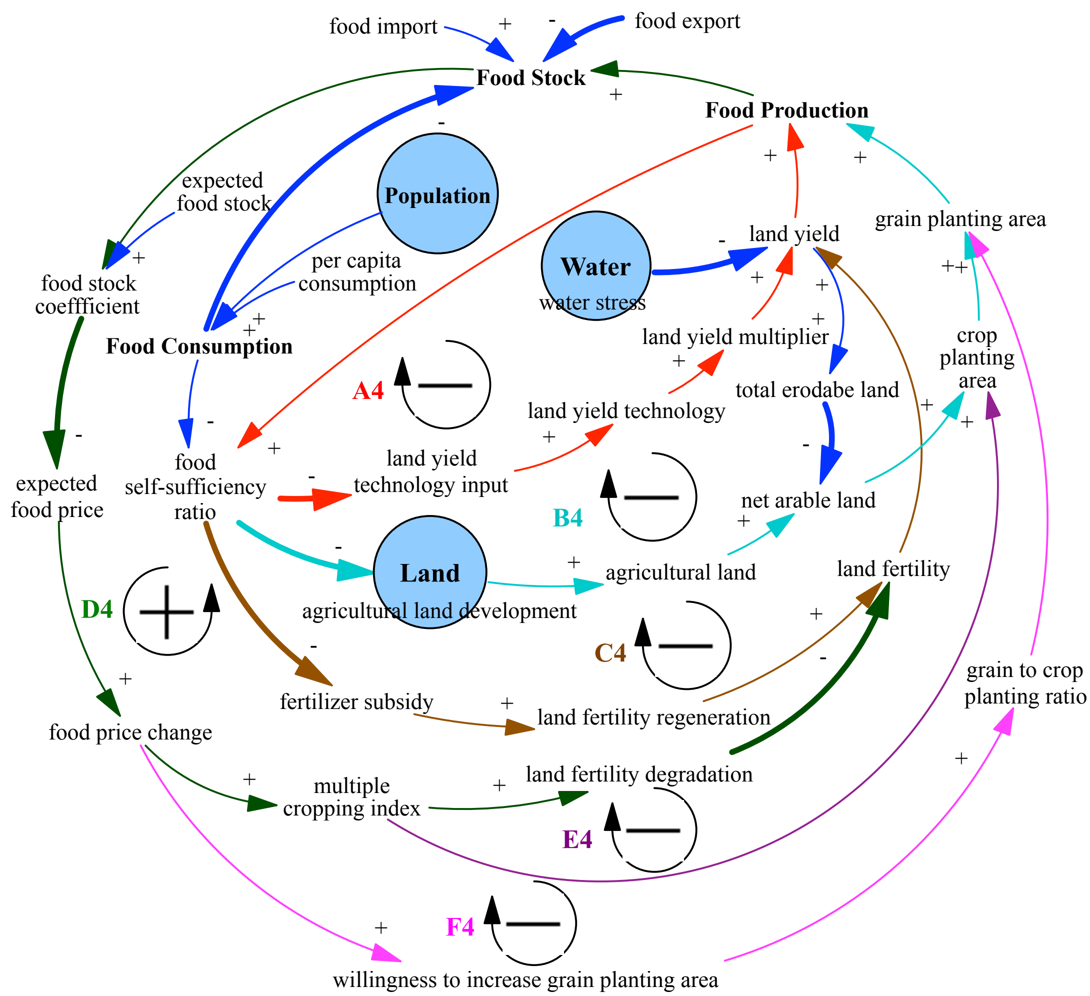

Figure 6. CLD in *Food Sector*

3.2.5 CLD in *Energy Sector*

Figure 7 shows the CLD in *Energy Sector*. Energy capital orders respond to two pressures. Orders first replace depreciation (loops A5 and B5). Loop A5 depicts the process of depreciation, which slowly depletes *energy capital* stock. Loop B5 compensates for depreciation by factoring it into *desired energy capital under construction*. Loop C5 moves *energy capital* from construction phase to completion phase. Orders then correct the gap between desired and actual *energy capital* (loop D5). *Desired energy capital* stock is anchored on actual *energy capital* stock and adjusted for *energy production pressure* (E5, which depicts the effect of *energy production pressure* on *energy capital*). Technology plays essential role in the *Energy Sector*. *Energy technology* on the one hand increases *energy production* for the same level of inputs of *energy capital* (loop G5); on the other hand, significantly lowers the intensity of *energy consumption per unit GDP* (loop H5).

Loop F5 illustrates the impact of resource depletion on *energy production*. Energy resources gradually deplete as more energy is produced. See also Fiddaman (1997) and Breach (2020) for detailed process of and mechanism behind the CLD in *Energy Sector*.

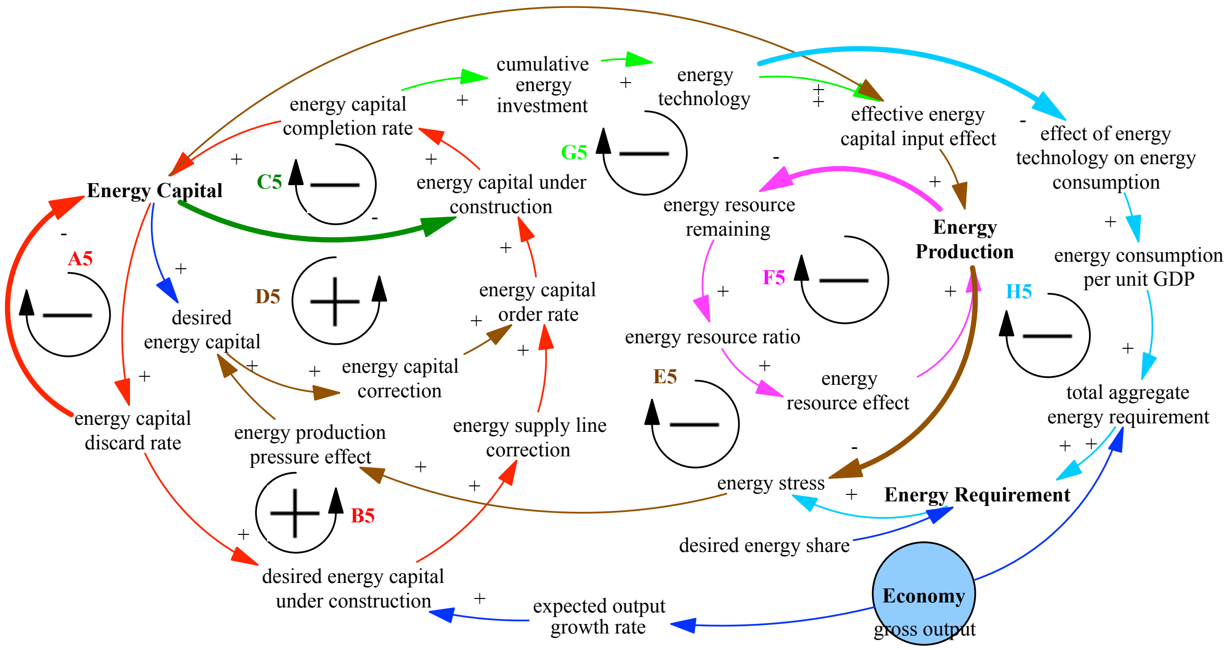

Figure 7. CLD in *Energy Sector*

3.2. 6 CLD in *Water Sector*

Figure 8 shows the CLD in *Water Sector*. Water supply capital orders respond to three pressures. Orders first replace depreciation (loops A6 and B6). Loop A6 depicts the process of depreciation, which slowly depletes *water supply capital* stock. Loop B6 counteracts loop A6 by factoring it into *desired water capital order rate*. Orders then correct the gap between desired and actual *water supply capital*. *Desired water supply capital* stock is anchored on actual capital stock and adjusted for *water stress* (loops C6, D6, and E6). Loops C6, D6, and E6 counteract *water stress* by prompting investment in *water supply capital* to increase water supplies in the form of *surface water*, *groundwater*, and *treated returnable waters*, respectively. Finally, orders augment *water supply capital* stock in order to anticipate output growth. Loop F6 illustrates the movement of water from atmosphere to surface as *precipitation* and then back to atmosphere through *evapotranspiration*. Loop G6 depicts the effect of *discharge* on *groundwater*. See also Breach (2020) for detailed mechanism behind the CLD in *Water Sector*.

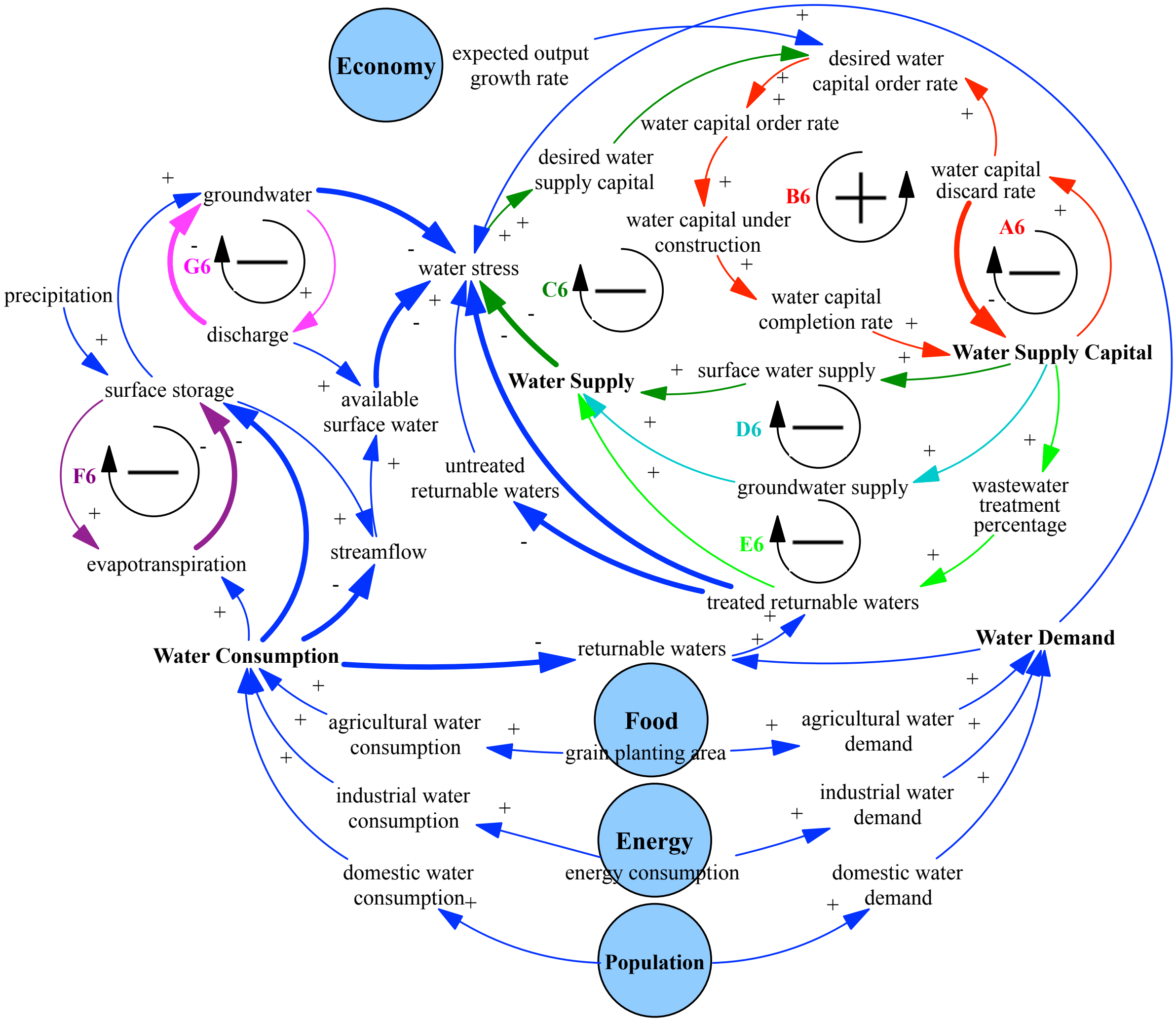

Figure 8. CLD in *Water Sector*

3.2.7 CLD in *Carbon Sector*

Figure 9 shows the CLD in *Carbon Sector*. The chain of negative loops passing through each of the terrestrial carbon stocks from the *biomass* to *litter*, to *humus*, and to *stable humus and charcoal* (A7, B7, C7) and the negative loops depicting the decaying (E7, G7, H7, I7) and burning (D7, F7) process of each carbon stock all act as a positive loop in the atmosphere-terrestrial carbon cycle (K7 and J7). An increase in atmospheric carbon results in higher uptake of carbon in the *biomass* through the effect of *net primary productivity*, which results in a greater transfer of carbon through the chain (*biomass*, *litter*, *humus*, *stabilized humus and charcoal*), thereby leading to an increase in decay and transfer of carbon back to the atmosphere. See also Goudriaan and Ketner (1984), Davies and Simonovic (2010, 2011), and Breach (2020) for the detailed mechanism behind the CLD in *Carbon Sector*.

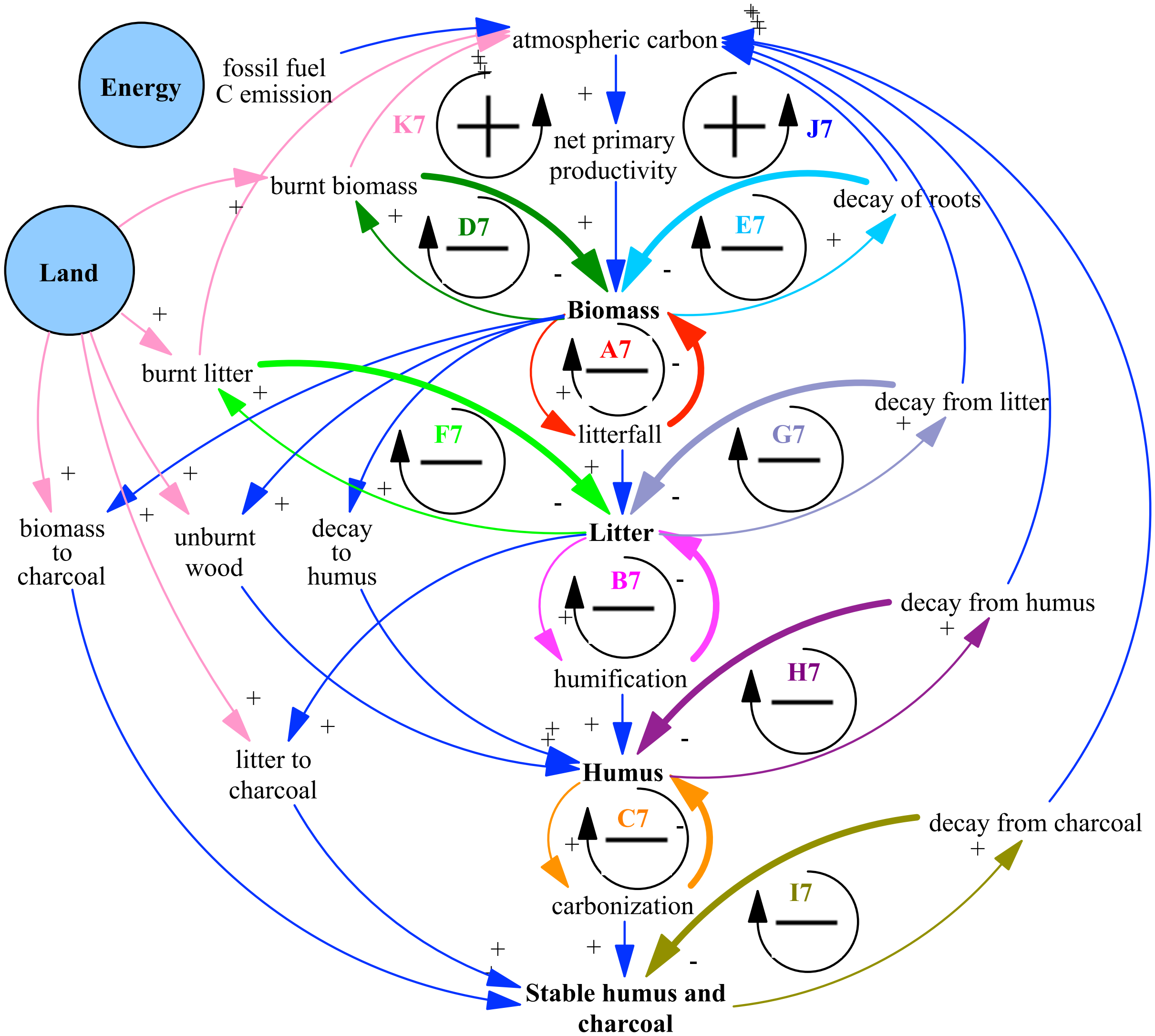

Figure 9. CLD in *Carbon Sector*

3.2.8 CLD in *Nutrient Sector*

Figure 10 shows the CLD in *Nutrients Sector*. The cycles of phosphorous and nitrogen follow that of the carbon cycle. Take a phosphorous cycle for example, the chain of negative loops passing through *land biota* to *humus* and to *rivers* (A8, B8, C8, D8, E8) and the negative loops depicting the *weathering of inorganic P* (F8) act as a positive loop in the terrestrial phosphorous cycle (G8). Because it represents a continuous cycle of negative feedback, it will attempt to reach equilibrium under natural conditions. Anthropogenic influences on this system in the form of wastewater discharge affect this equilibrium and drive changes in the nutrient cycles. See also Mackenzie et al. (1993) and Breach (2020) for the detailed mechanism behind the CLD in *Nutrient Sector*.

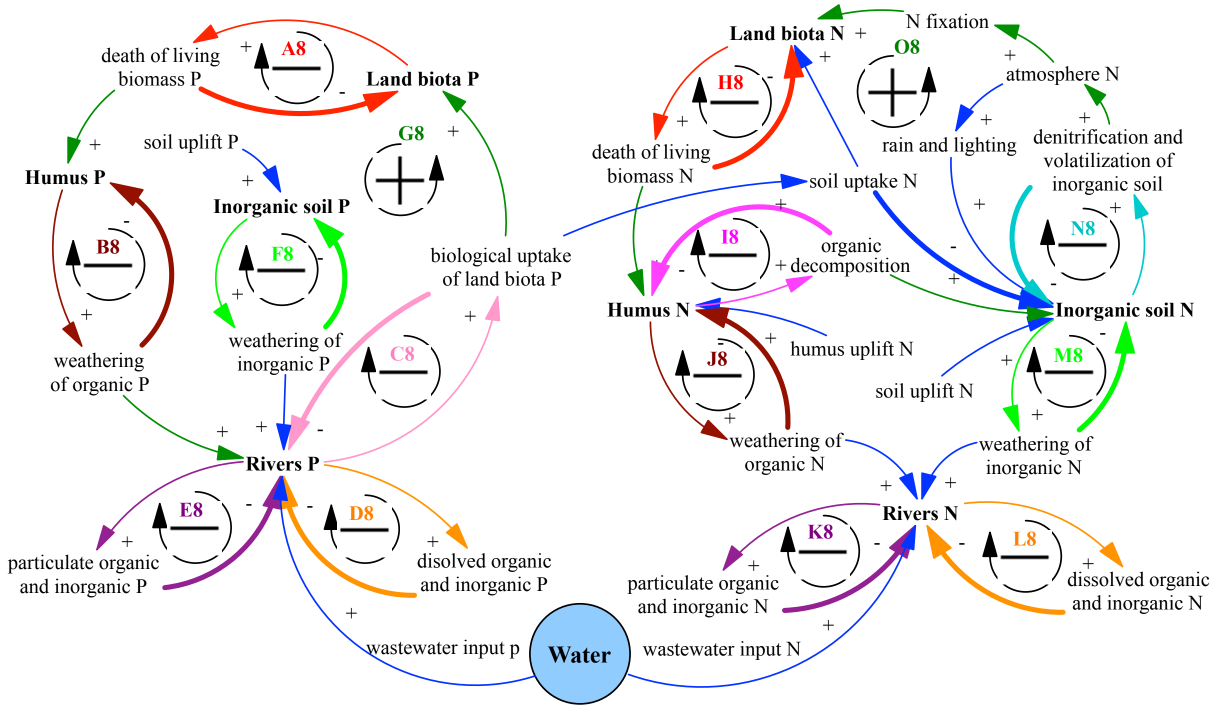

Figure 10. CLD in *Nutrient Sector*

3.2.9 CLD in *Fish Sector*

Four feedback loops drive the dynamics of *fish biomass stock* (Figure 11). Loops A9, C9, and D9 represent negative feedback on *fish biomass stock* through *natural fish death*, *fish recruits*, and *fish yield*, respectively. The amount of wastewater water acts as a positive factor on *natural mortality*. Loop B9, which connects *total reservoir capacity* and *ship cargo volume* with *fish birth rate*, acts as positive feedback on *fish biomass stock*. As *total reservoir capacity* and *ship cargo volume* increase, *fish birth rate* decreases so too does the *fish birth*. The decline in *fish birth* decreases *fish biomass stock*, further reducing *fish birth*.

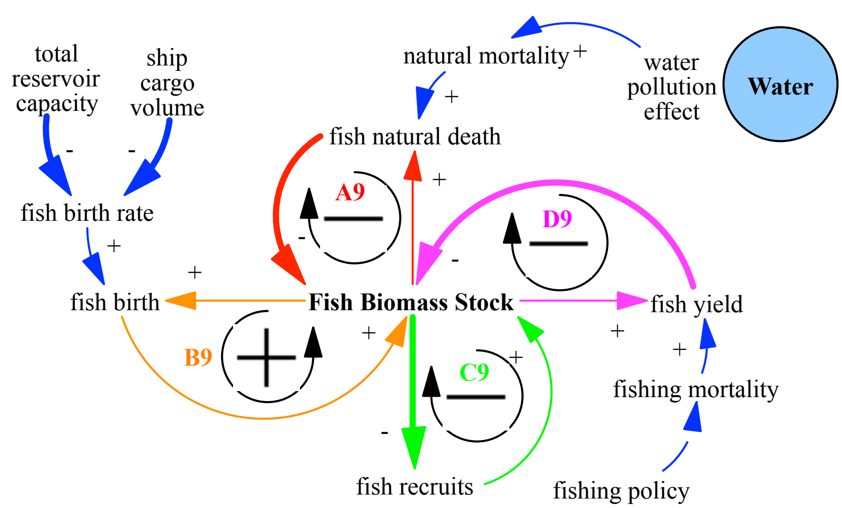

Figure 11. CLD in *Fish Sector*

4. ANEMI_Yangtze: model development

4.1 The ANEMI_Yangtze data system

The ANEMI_Yangtze data system contains (i) historical data that is used to initialize and validate the model and (ii) future parameters that govern changes in the future. Most of the historical data (1990-2015), such as population and GDP, energy production and consumption, food production and food trade, and water withdrawals and consumptions, come from the Statistical Yearbook published by the National Bureau of Statistics of China annually (available on line at http://www.stats.gov.cn/english/, last accessed May 16, 2022). Historical precipitation, evapotranspiration, and temperature data are collected from hydrometeorological stations. Land use data come from ESA Climate Change Initiative - Land Cover (http://maps.elie.ucl.ac.be/CCI/viewer/, last accessed May 16, 2022). Adjustments are made to the historical data as needed to fill in the missing information. Future temperature and precipitation data come from Yu et al. (2018). For future parameters, the ANEMI_Yangtze data system uses information about technology cost and performance, information about future development policies, as well as the authors' experience of knowledge. Additional information on the data is also described in the sections below.

4.2 Major changes: a glimpse

ANEMI_Yangtze is developed based on ANEMI3, which has its roots in the *WorldWater* by Simonovic (2002, 2002a). ANEMI has been updated continuously from its first publication in 2010 (Davies and Simonovic, 2010) to the most recent edition in 2021 (Breach and Simonovic, 2021). The current version of ANEMI consists of the following twelve sectors that reproduce the main characteristics of the climate, carbon, population, land use, food production, sea-level rise, hydrologic cycle, water demand, energy-economy, water supply development, nutrient cycles, and persistent pollution. In ANEMI_Yangtze, hydrological cycle, water demand and water supply development, as well as wastewater discharge and treatment, are all integrated in *Water Sector*. Climate change is not explicitly simulated. Instead, we use exogenous precipitation and temperature to drive the hydrological cycle. Sea level rise and persistent pollution are excluded. The global cycles of carbon, nutrients, and hydrology are tailored to fit a regional context. A new *Fish Sector* is added since fisheries are important for regional economy and diet. Major modifications are in *Population*, *Food*, *Energy*, and *Water Sectors*. Due to space limitation, only new aspects of the model are described in detail. For further information about the model, please refer to ANEMI_Yangtze's technical report from Jiang and Simonovic (2021) and Dr. Breach's PhD dissertation (Breach, 2020).

4.3 Population

Births, *deaths*, and *migrants* are the three variables drive the dynamic behaviour of the Belt's population. Figure 12 shows the stock and flow diagram in *Population Sector*. Population is split into three age demographics to allow for working population (ages 15 to 64) to represent *labor force* in the economic model. The ageing chain of population groups can be represented as:

$$\begin{cases} P_{0-14} = \int \left(B + netM_{0-14} - P_{0-14} \cdot M_{0-14} - \frac{P_{0-14}(1-M_{0-14})}{\tau_1} \right) dt \\ P_{15-64} = \int (netM_{15-64} + \frac{P_{0-14}(1-M_{0-14})}{\tau_1} - P_{15-64} \cdot M_{15-64} - \frac{P_{15-64}(1-M_{15-64})}{\tau_2}) dt \\ P_{65+} = \int (netM_{65+} + \frac{P_{15-64}(1-M_{15-64})}{\tau_2} - P_{65+} \cdot M_{65+}) dt \end{cases} \tag{1}$$

Where P_i is population, $netM_i$ is *net migrans*, M_i is *mortality*, τ_i is length of time spent in sub-demographic. *B* represents *births* and is calculated as,

$$B = TF \cdot \frac{FM_r \cdot P_{15-49}}{R_{life}} \tag{2}$$

Where FM_r is *female ratio* (its value usually lower than 0.5 due to the well-known phenomenon of "missing girls", a side-effect of the one-child policy), $P_{15\text{-}49}$ is the population between age 15-49, R_{life} is *reproductive lifetime* of 30 years. *TF* is *total fertility*, which is determined by a number of factors, including *fertility control effectiveness*, capital allocation, and *desired family size*. Its calculation (equation (3)) is adapted from ANEMI3 (Breach, 2020).

$$TF = MIN(MTF, (MTF \cdot (1 - F_{control}) + DTF \cdot F_{control})) \tag{3}$$

where *TF* is *total fertility*, *MTF* is *maximum total fertility*, $F_{control}$ is *fertility control effectiveness*, *DTF* is *desired total fertility*.

Life expectancy, which determines *mortality*, is affected by both economic and environmental factors. The calculation of *life expectancy* is adapted from Ma and Yu (2009). At the regional scale, vital resources such as food and water can be traded, so in ANEMI_Yangtze, only the effect of pollution is considered. The empirical relationship between *mortality* and *life expectancy* is adopted from ANEMI3 which originally adopts from Meadows et al. (1974).

$$L_E = (L_{EN} + a \ln GDP_{per} + b \ln EHS_{per}) Pollution_{multi} \tag{4}$$

$$Pollution_{multi} = c \cdot PI^2 + d \cdot PI + e \tag{5}$$

$$PI = \sqrt{\frac{N_I}{N_{I0}} \cdot \frac{P_I}{P_{I0}}} \quad (6)$$

Where L_E is *life expectancy*, L_{EN} is *life expectancy normal*, GDP_{per} is *GDP per capita*, EHS_{per} is *effective health service per capita*, $Pollution_{multi}$ is *lifetime multiplier from pollution*, *PI* is *pollution index*. N_I (P_I) and N_{I0} (P_{I0}) are the simulated and initial nitrogen (phosphorous) concentration. *a*, *b*, *c*, *d*, and *e* are calibrated parameters.

Migration is newly added. According to Lee (1966), economic factors are mainly responsible for migration. In China, the most important factor driving migration in the 1980s (post-reform period) is the institutional driver and then the economic driver dominants afterwards (Shen 2013). Apparently, policy on migration can't be ignored considering China's central-planning logic and mechanisms. We thus introduce a *migration policy* factor to account for the institutional barrier and suppose its value ranges from 0-1, with bigger value indicating policy that is in favor of migration. Social environment is also an intermediate factor affecting migration (Lei et al., 2013). In China, most minorities (China's 56 ethnic groups) live in areas with the same or similar language and culture as well as eating habits and are very reluctant to move (Su et al., 2018). Therefore, we employ a factor - *migration willingness* - which is calculated as the proportion of the minorities to account for the "border effect" in migration. Research also finds that economic prosperity can not only attract labour migration, but also restrain population inflows in megacities due to high housing prices (Zhao and Fan, 2019). This research introduces a *crowding factor* affected by *settlement area per capita* to account for house price impact. The calculation of *migration rate MR* is thus formulated as:

$$MR = F_{GDP\,diff} \cdot MW \cdot MP. F_{crowding} \quad (7)$$

where $F_{GDP\,diff}$ is *GDP difference factor*, which is used to calculate the difference between *GDP per capita* in the upper, middle, and lower Yangtze Economic Belt and *GDP per capita* in the Belt. This means only the migration within the Belt is considered (*i.e.*, people migrate from the less developed upper and middle Belt to the developed lower Belt). *MW* is *migration willingness*. *MP* represents *migration policy* and the value of 1 is adopted in this research. $F_{crowding}$ is a *crowding factor* and is affected by *settlement area per capita*.

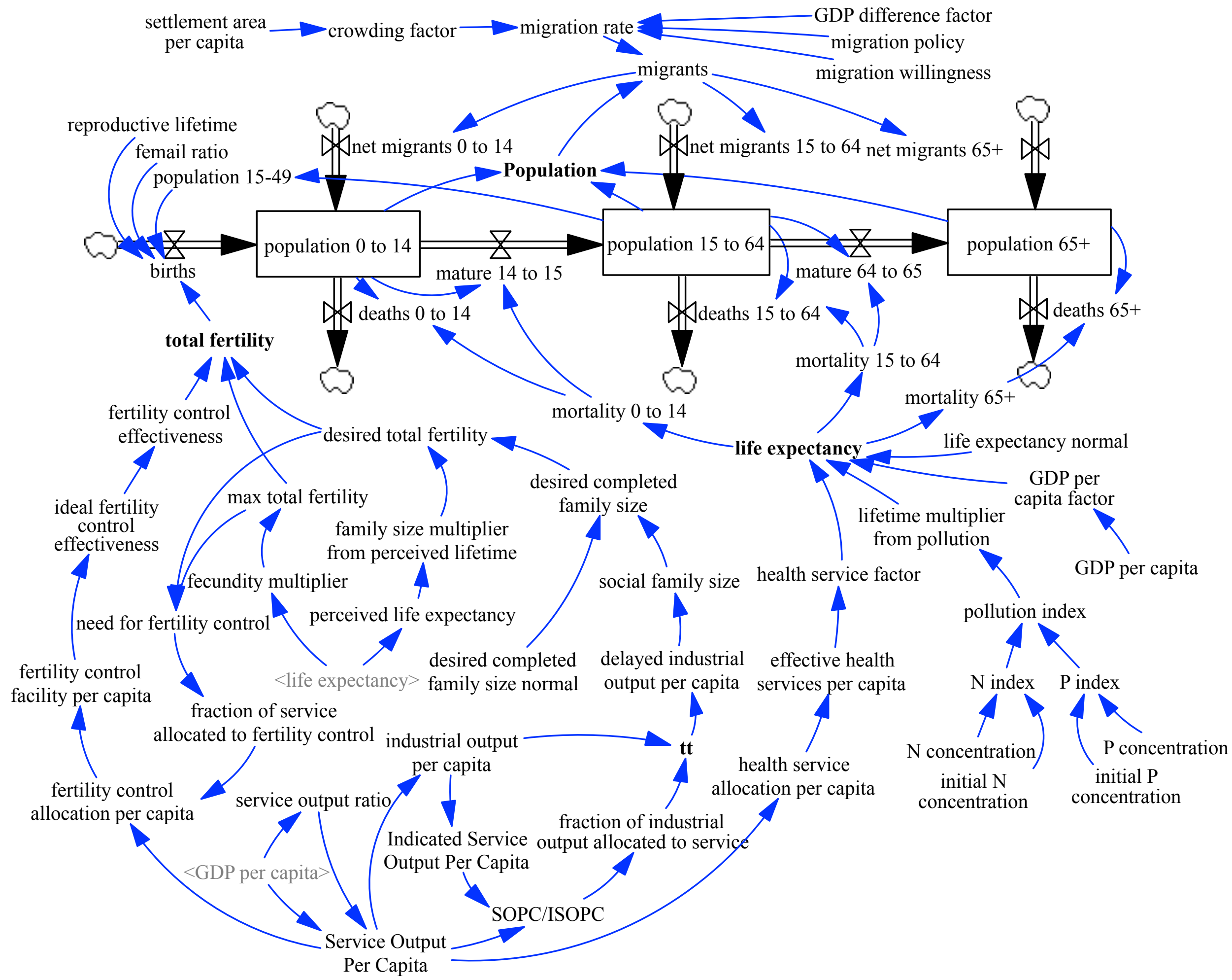

Figure 12. Stock and flow diagram of the *Population Sector*

4.4 Food

The *Food Sector* of ANEMI_Yangtze calculates the production and consumption of food and *food import/export*, and its stock and flow diagram is shown in Figure 13. *Food consumption* is the production of *population* and *per capita food consumption*. In ANEMI_Yangtze, *per capita food consumption* is assumed to be 400 kg/year/person throughout the simulation. *Food production* is affected by several factors, including *land fertility*, *arable land*, and *water stress*. Its dynamic behaviour is mainly driven by the difference between *perceived* and *desired food self-sufficiency*. *The food self-sufficiency* index is defined as the ratio of *food production* to *food consumption*. When its value declines below 0.95 (a critical value) incentives for *land yield technology input*, *agricultural land development*, and *fertilizer subsidy* shall be provided to ensure food security (Ye et al., 2013).

$$FP = LY \cdot GPA \cdot (1 - Loss) \tag{8}$$

$$LY = LF \cdot LY_{multi} \cdot F_{WS} \quad (9)$$

where *FP* is *food production*, *LY* is *land yield*, *GPA* is *grain planting area*, *Loss* represents *processing loss*. *LF* is *land* fertility, LY_{multi} is *land yield multiplier*, F_{WS} represents *water stress to land yield factor*.

The *Food Sector* also enables food trade, *i.e*., *food import* and *food export*, which is affected by *local food price* and *international food price* and its calculation is adapted from Wang et al. (2009).

$$FIE = F_{pop} \cdot f_1 + f_2 \cdot FP - f_3 \cdot IFP \quad (10)$$

Where *FIE* is *food import*/*export*, with positive *FIE* indicating import and negative ones export. F_{pop} is population rescale factor, approximately equals to the ratio of the Belt's population to the national total population. *FP* is *food price* and *IFP* is *international food price*. The historical values of *IFP* are from FAO (http://www.fao.org/worldfoodsituation/foodpricesindex/en/, last accessed May 16, 2022). The future values are set to the base year 2015 values. f_i is calibrated parameter. *Food price* is simulated as a stock variable and accumulates by *food price change*, which is another important factor affecting *food production* through influencing farmers' adopting of multiple cropping practices (*multiple cropping index*) and increasing of *grain planting area*.

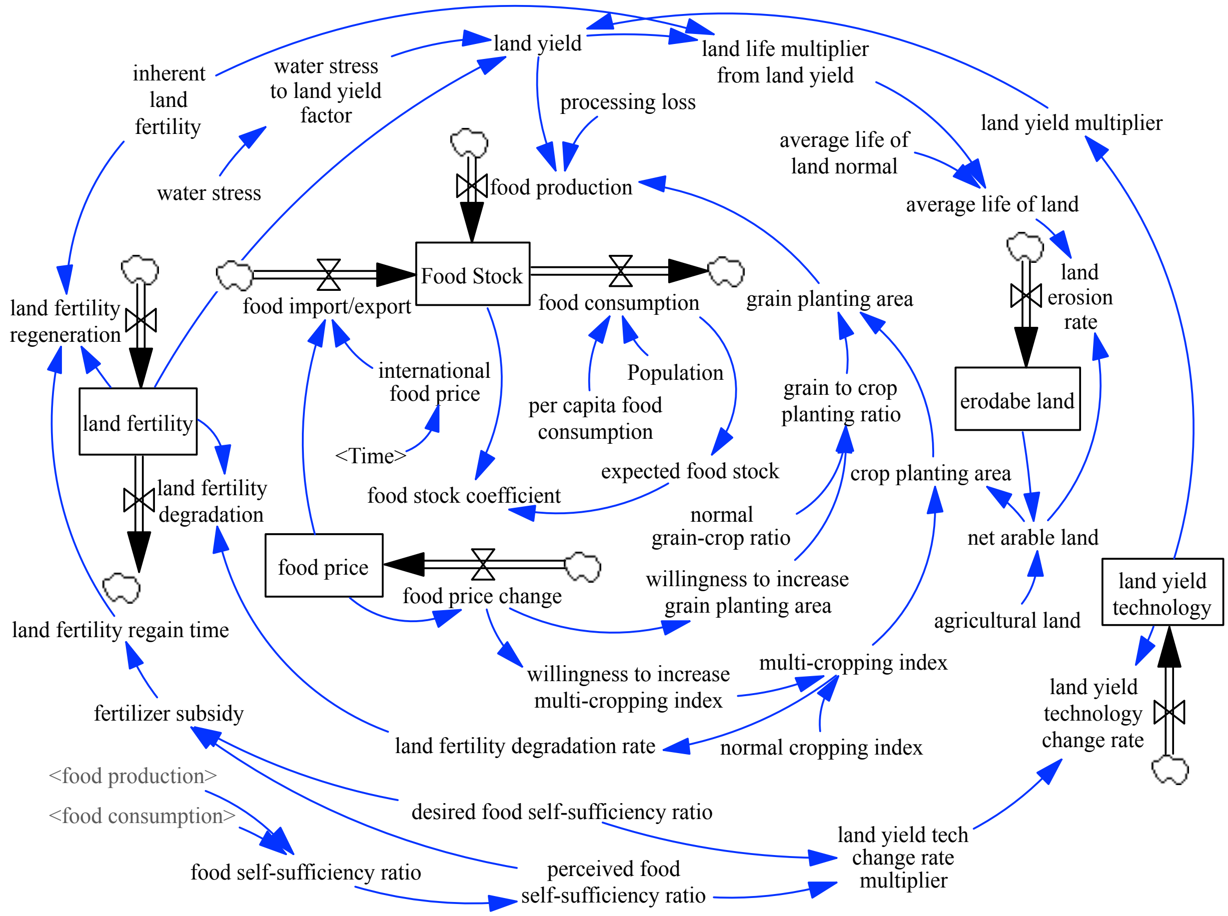

Figure 13. Stock and flow diagram of the *Food Sector*

4.5 Energy

The energy system of ANEMI_Yangtze includes the representation of *energy capital* development, *energy technology*, and *energy requirement*, *production*, and *consumption*. Figure 14 shows the stock and flow diagram of the *Energy Sector*. Six primary energy resources, three renewable sources (hydropower, nuclear, and new energy sources) and three non-renewable sources (coal, oil, and gas) are considered. *Energy capital* is energy production capital stock. It is represented as developed field or mine for fossil fuels and built plants for nuclear and hydropower. The formulations of *energy capital* (KE_i) and *energy capital under construction* (KEC_i) are the same as those in ANEMI3 (Breach, 2020: equations (3.52), (3.53)). For simplicity, we do not simulate the effect of return on *energy capital* which is determined by energy capital cost and the marginal product of energy capital in ANEMI3. We thus formulated the calculation of *desired energy capital order rate* as,

$$DKEO_i = \frac{KE_i}{\delta_i} + \frac{DKE_i - KE_i}{\tau_c} + \frac{DKEC_i - KEC_i}{\tau_s} \quad (11)$$

$$DKEC_i = \frac{KE_i}{\delta_i} + GR_{GDP} \cdot KE_i \cdot delay_C \quad (12)$$

The first term on the right-side of the formula represents *energy capital discard rate* in which KE_i is *energy capital*, δ_i is *energy capital lifetime*. The middle term represents *energy capital correction* in which DKE_i is *desired energy capital*, equaling to current *capital* adjusted for *production pressure.* The pressure effect of energy production is treated as a look-up table function of *energy stress*. *Energy stress* is defined as the ratio of *energy requirement* to *energy production*. τ_c is correction time for *energy capital*. The third term represents correction to supply line of *energy capital under construction* in which $DKEC_i$ and KEC_i are desired and current *energy capital under construction*. $DKEC_i$ equals quantity needed to replace discards and meet growth and is fumulated as equation (12), in which GR_{GDP} is expected growth rate of *gross output*, $delay_C$ represents the time required to construct new *energy capital*. τ_s is correction time for supply line of *energy capital under construction. i* denotes the six energy sources.

The *total aggregate energy requirement* in ANEMI_Yangtze scales with economy and is represented as the production of *gross output* and *energy consumption per unit GDP*. *Energy requirement* by sources is the production of *total aggregate energy requirement* and *desired energy share* (which is exogenously specified).

Three factors affect *energy production* for each source: *energy capital*, *energy technology*, and resources effect. The supply of producing capital is mainly driven by the pressure effect of energy production, *i.e.*, *energy stress* (defined as the ratio of *energy requirement* to *energy production*). Resource effect affects *energy production* through depletion and saturation. Depletion effect represents the diminishing productivity of nonrenewable energy production as the resource remaining declines and saturation refers to diminishing returns to production effort for the renewable energy. Technology increases *energy production* for the same level of inputs of *energy capital* through learning process usually called as an endogenous learning curve, with cumulative investment in *energy capital* as its input. The formulation of *energy production* is the same as in ANEMI3 (Breach, 2020: equations (3.49)) which is based on Fiddaman (1997).

Energy price in ANEMI3 is endogenously simulated, whereas in ANEMI_Yangtze it is exogenously specified, with historical prices from China Customs Head Office and China Energy Statistical Yearbook and future prices assumed to remain their 2015 base year values.

Energy consumption equals to *energy requirement* by assuming that requirement can always be met through production and trade. Energy trade is not simulated in this research.

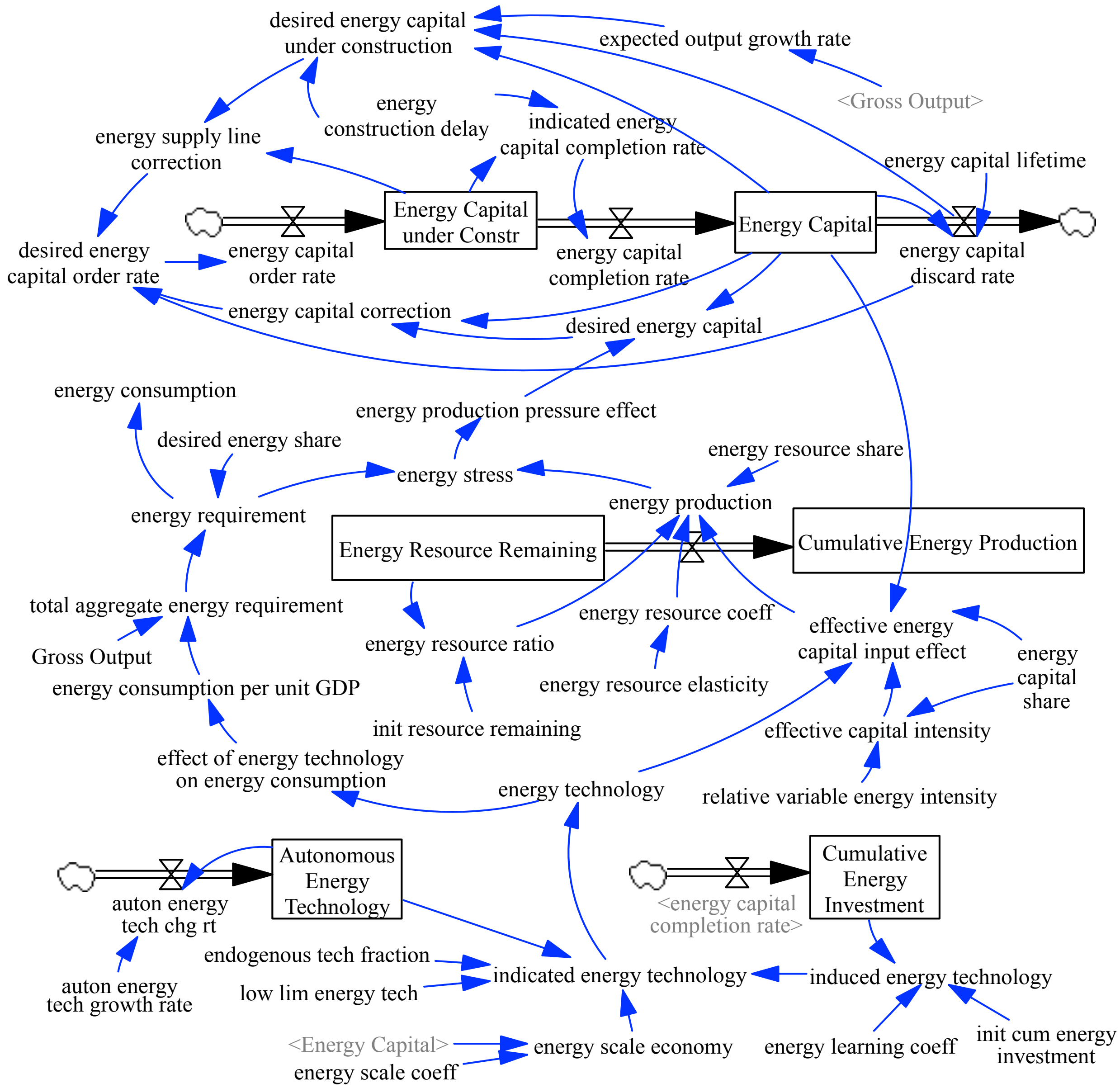

Figure 14. Stock and flow diagram of the *Energy Sector*

Table 1 shows the endowments of the six energy sources. Reserves for renewables mean the upper limit to renewable output. The upper limit for hydropower is based primarily on the hydro endowment, nuclear potential implicitly assumed to be politically limited, and new energy is the sum of wind and solar potentials.

Table 1 Energy endowments in the Belt

Type	Energy source	Reserves	Unit	Source

non-renewables	coal	128.556	billion tce	Yao et al. 2020
	oil	0.460	billion tce	Fang et al. 2018
	gas	19.188	billion tce	Fang et al. 2018
renewables	hydropower	0.379	billion tce/year	Liu and Ding, 2013
	nuclear	0.134	billion tce/year	SGERI and CNPD 2019
	new	318.386	billion tce/year	Song 2013; Zhu et al. 2006

4.6 Water

Water Sector consists of the hydrological cycle, *water demand*, *desired water consumption*, water supply development, as well as wastewater discharge and treatment. Figure 15 shows the stock and flow diagram of the *Water Sector*.

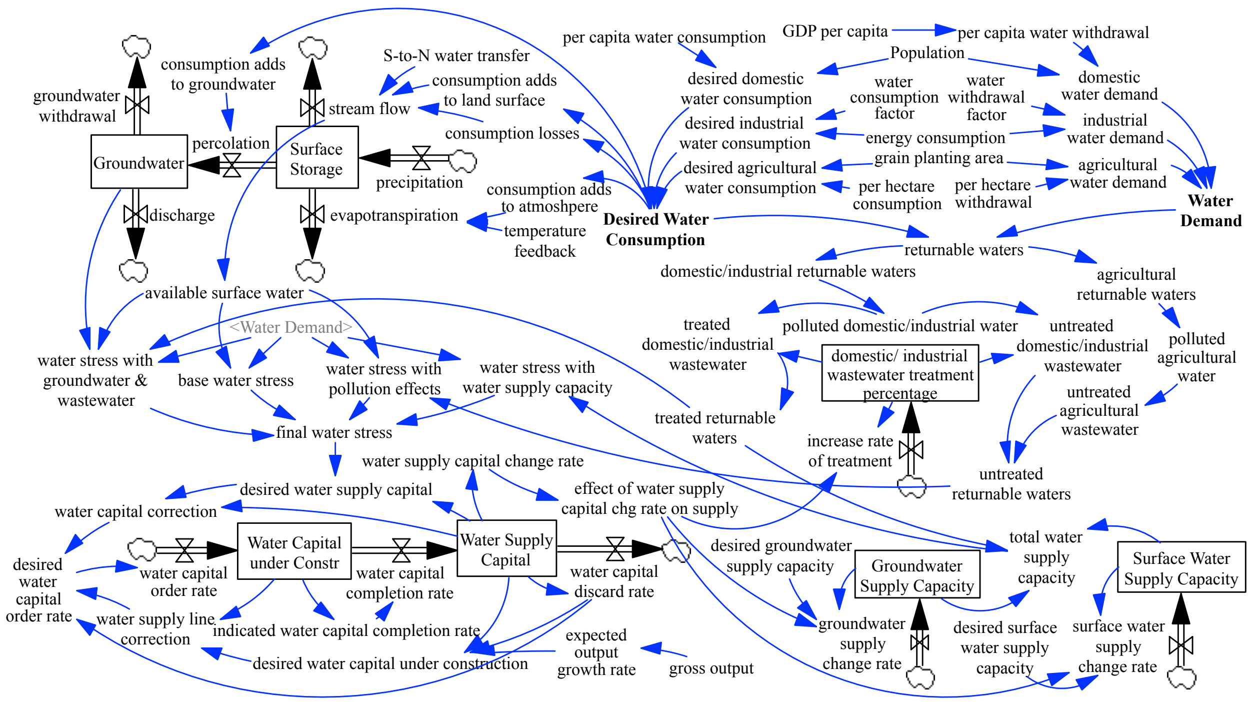

Figure 15. Stock and flow diagram of the *Water Sector*

The hydrological cycle describes the flow of water from atmosphere in the form of *precipitation* to land *surface storage* and through *groundwater* back to East China Sea. The South-to-North water transfers (west, middle, and east lines) and *water consumption* are also considered. The water balance equations in the Belt are as follows,

$$SS = \int (Pre - ET - Per - SF)dt \qquad (13)$$

$$GW = \int (Per - GWW - Dis)dt \qquad (14)$$

$$Per = a\left(\frac{SS}{SS_0}\right) + CS_{gr} \qquad (15)$$

$$SF = b(\frac{SS}{SS_0})^2 - CS_{at} - CS_{ls} - CS_{gr} - CS_{loss} - S2N \quad (16)$$

$$Dis = c\left(\frac{GW}{GW_0}\right) \quad (17)$$

Where *SS* is *surface storage*, *Pre* is *precipitation*, *ET* is *evapotranspiration*. *Per* and *SF* represent *percolation* and *stream flow* and are formulated as equations (15) and (16), respectively. CS_{at}, CS_{ls}, CS_{gr}, and CS_{loss} represent respectively the water *consumption adds to atmosphere*, *landsurface*, *groundwater*, and *consumption loss*. *S2N* is the South-to-North water transfer. *a*, *b*, and *c* are calibrated parameters. *GW* is *groundwater*, *GWW* represents water withdrawn from groundwater storage, *Dis* means groundwater discharge and is formulated as equation (17).

The calculation of *domestic* and *agricultural water demands* and consumptions is the same as in ANEMI3. *Industrial water demand* is dominated by the generation of electricity, which consists of both non-renewable sources (coal-fired and gas-fired thermal power) and renewable sources (hydropower and nuclear power). The *water withdrawal factor* and *water consumption* of thermal energy vary substantially among different cooling methods and their values for different fuel sources are obtained from Zhang et al. (2016) and shown in Table 2. Nuclear power plants in the Belt are located in coastal areas and rely on seawater for cooling, so the freshwater withdrawal and consumption factors of nuclear power are all set to zero. The calculation of *electricity water demand* takes the following form.

$$W_{ele} = Tech_{ele}.\sum_{i=1}^{4} E_{P_i} \cdot \sum_{j=1}^{n} WWF_{i,j} \cdot F_{i,j} \quad (18)$$

where W_{ele} is *electricity water demand*; E_{Pi} is *electricity production* for energy source *i*; WWF_i is *water withdrawal factor* for energy source *i*; $F_{i,j}$ is the fraction of cooling method *j* for energy source *i* and is externally prescribed; $Tech_{ele}$ is technological change for withdrawals in *electricity production* and is also exogenously specified. *Industrial water demand* is calculated as,

$$W_{ind} = \frac{1}{R_{ele}} \cdot W_{ele} \quad (19)$$

where W_{ind} is *industrial water demand*; R_{ele} is the ratio of *electricity water demand* to *industrial water demand* and is set to 0.7 in this research.

Table 2 Water withdrawal and consumption factors for electricity production

Energy source *i*	Cooling method *j*	Water withdrawal factor (m^3/MWh)	Water consumption factor (m^3/MWh)
Coal	OT	98.54	0.393

	RC	2.466	1.972
	DRY	0.438	0.448
Gas	OT	34.07	0.379
	RC	2.902	2.114
Nuclear	OT (seawater)	178	1.514
Hydro		0	0

Note: OT=once through, RC=recirculating

In ANEMI_Yangtze, water demand is defined as the amount of water needed for the domestic, industrial, and agricultural sectors. We calculate water consumption as the desired consumption assuming that consumption and withdrawal can always be met, which means we do not simulate the unsatisfied demand directly. Instead, we use *water stress* as a measure of water shortage. The definitions and formulations of *water stress* are described in the following section.

Three supply types: surface water, groundwater, and wastewater reclamation are considered. The production of water supplies is driven economically by investing in *water supply capital* stocks for each source. The structure and formulation of water supply development follow that of the energy capital development. Similarly, the effect of *water stress* is introduced as an indicator for *water supply capital* investment and has four definitions (a value bigger than 1 indicting water shortage). The *base water stress* WS_{base} is represented as,

$$WS_{base} = \frac{W_{dom}+W_{ind}+W_{agr}}{SW_{avai}} \quad (20)$$

where SW_{avai} is *available surface water*, which is the stable and reusable portion of the total renewable streamflow..

The *water stress with groundwater and wastewater* WS_{gw+ww} is represented as,

$$WS_{gw+ww} = \frac{W_{dom}+W_{ind}+W_{agr}}{SW_{avai}+r_{gw}\times GW+TRW} \quad (21)$$

where r_{gw} is *groundwater use ratio*, set to 0.01 based on the ratio of historical groundwater withdrawals to total withdrawals; *GW* is *groundwater*; *TRW* is *treated returnable waters*.

The *water stress with pollution effects* $WS_{pollution}$ is represented as,

$$WS_{pollution} = \frac{W_{dom}+W_{ind}+W_{agr}}{SW_{avai}-f_{ww}\times UTRW} \quad (22)$$

where f_{ww} is *wastewater pollution factor*, set to 8 (based on Shiklomanov (2000)); *UTRW* is *untreated returnable waters*.

The *water stress with water supply capacity* WS_{supply} is represented as,

$$WS_{supply} = \frac{W_{dom}+W_{ind}+W_{agr}}{TWS} \quad (23)$$

where *TWS* is *total water supply capacity*, which is the sum of *surface water supply capacity*, *groundwater supply capacity*, and *treated returnable waters*.

4.7 Fish

The *Fish Sector*, which is an entirely new addition to ANEMI_Yangtze, is used to simulate the dynamic of *fish biomass stock* over time. Figure 16 shows the stock and flow diagram of the *Fish Sector*.

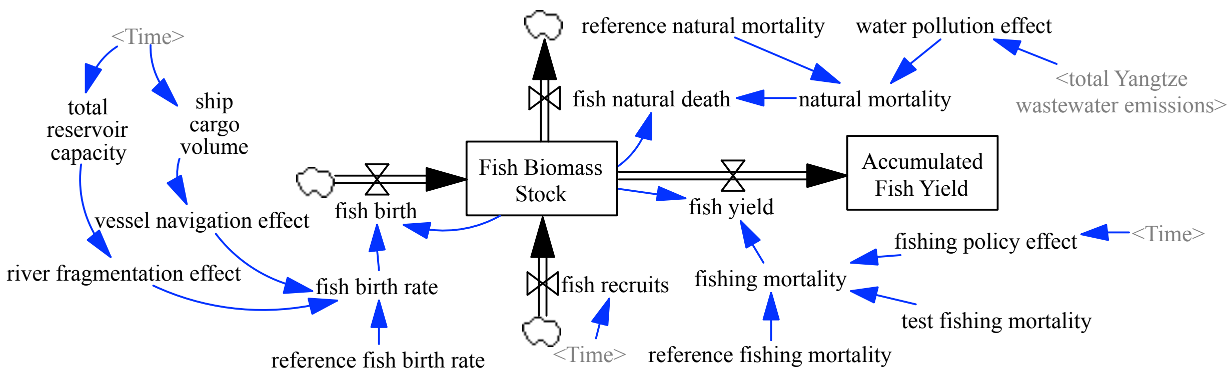

Figure 16. Stock and flow of the *Fish Sector*

The calculation of *fish biomass stock* is given as,

$$F = \int \left(f_b + f_r - f_d - f_y\right) dt \quad (24)$$

where F is *fish biomass stock*, f_b is *fish birth*. f_r represents *fish recruits*, which is treated as an exogenous variable. f_d is *natural fish death*, f_y is *fish yield*.

Fish catch data come from Zhang et al. (2020). Major parameters in the *Fish Sector* are given in Table 3.

Table 3 Major parameters and their corresponding values in the *Fish Sector*

Variable	Value	Unit	Source
reference natural mortality	0.075	dmnl	Gilbert et al. (2000)
reference fishing mortality	0.7949	dmnl	Chen et al. (2009)
reference fish birth rate	0.826	dmnl	Zhang et al. (2020)

Note: for *reference fishing mortality* the value of 0.7949 is calculated based on Chen et al. (2009) by averaging the exploitation coefficients of 10 economic fish species (fishing mortality = 0.761, 0.706, 0.803, 0.829, 0.898, 0.876, 0.846, 0.774, 0.765 and 0.691). For *reference fish birth* *rate* the value of 0.826 is calculated based on Zhang et al. (2020) by averaging fish growth rates in the middle Yangtze reach, Dongting lake, and Poyang lake.

5. Model validation and application

5.1 Model validation and sensitivity analysis

The ANEMI_Yangtze model was validated by comparing simulated results with historical data for 1990-2015. The results shown in Figure 17 indicate that the model can reproduce the system behaviour very well for *population*, *gross economic output*, and *water demand* (Figure 17(a, b, and f)). The model can capture the general behaviour patterns for *energy requirement*, *energy production*, and *food production* (Figure 17(c-e)). The fluctuations of historical *food production* are mainly attributed to the flood and drought disasters, which are not currently captured by the model. The discrepancies between historical and simulated *energy requirement* and *energy production* are partly due to the previous energy policies acting on the energy system that the model doesn't consider. For example, in China, overcapacity in coal production gradually appeared after the mid-1990s, and this situation worsened after the outbreak of the 1997 Asian financial crisis. To alleviate the overcapacity crisis, the governments at all levels issued series of policies to reduce production, seen as the production drop around year 2000 (Figure 17(d)).

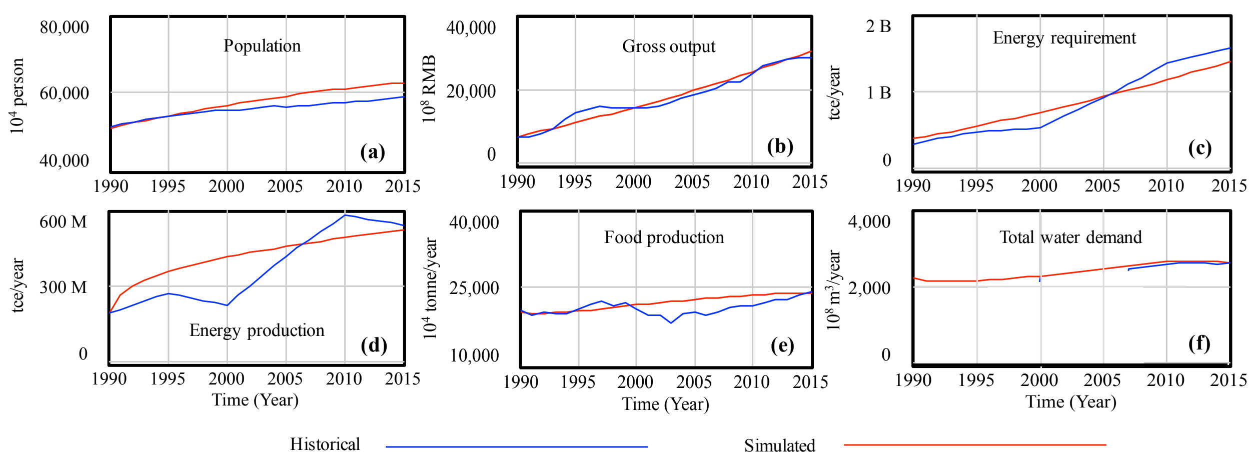

Figure 17. Comparison of simulated and historical system behaviour

Sensitivity analysis aims to build confidence in the model's ability to generate robust system behaviour by applying Monte Carlo simulation. The parameters used for sensitivity tests (shown in Table 4) are chosen due to uncertainty in their values. The selected parameters are varied by -10% ~ +10% (mild variation scenario) and -50% ~ +50% (extreme variation scenario) to determine whether the main state variables will exhibit alternative behaviour. Triangular probability distribution is used. The highest point of probability in the triangle is assigned to the baseline value of these parameters, where the outer limits are defined by the minimum and maximum percent changes of the value.

The sensitivity simulations are performed by considering all the possible parameter change combinations together, and the results are shown in Figure 18. The lowercase letters show the results for the mild variation scenario and the capital letters for the extreme variation scenario. As can be seen, the range of the projected variables becomes smaller with the decreasing of the confidence level. For each of the examined variables shown in Figure 18 (a-f), the behaviour modes remain the same within the range of the parameters tested when the variation is mild (-10% ~ +10%). When the variation is extreme (-50% ~ +50%), the range in the trajectory of the state variables is larger. However, the behaviour of each variable still remains the same (Figure 18 (A-F)). The lack of changes in behaviour modes while testing sensitivity is desirable, indicating that the model is robust.

Table 4 Parameters used for sensitivity tests of main state variables

State variable	Parameters	Baseline value	Unit
Population	normal life expectancy	52.5	year
	female ratio	0.5	dmnl
	reproductive lifetime	35	year
Gross output	value share of labor	0.6	dmnl
	capital energy substitution elasticity	0.75	dmnl
	capital lifetime	40	year
Food production	per capita food consumption	400	kg/year/person
	normal average life of land	6000	year
	inherent land fertility	6300	kg/hectare/ year
Energy production	energy resource elasticity [coal, oil, gas, hydro, nuclear, new]	0.625, 0.657, 0.657, 0.303, 0.303, 0.527	dmnl
	energy capital lifetime [coal, oil, gas, hydro, nuclear, new]	15, 15, 15, 30, 30, 20	year
	reference energy consumption per unit GDP	6	tce/10000rmb
Water demand	reference water withdrawal factor [coalOT, coalRC, coalDRY, gasOT, gasRC, hydro, nuclearOT]	98.54, 2.47, 0.44, 34.07, 2.90, 0, 0	m^3/MWh
	initial water intake	4000	m^3/hectare/ year
Nitrogen concentration	N leaching coefficient of agricultural runoff	18.65	kg/hectare/year
	N concentration of domestic wastewater	60	g/L
	N concentration of industrial wastewater	60	g/L

Note: The values of N concentration of domestic/industrial wastewater are from Henze and Comeau (2008), and the value of N leaching coefficient of agricultural runoff is obtained from FAO (http://www.fao.org/3/w2598e/w2598e06.htm, last accessed May 16, 2022). Energy resource elasticities are from ANEMI (Breach and Simonovic, 2021).

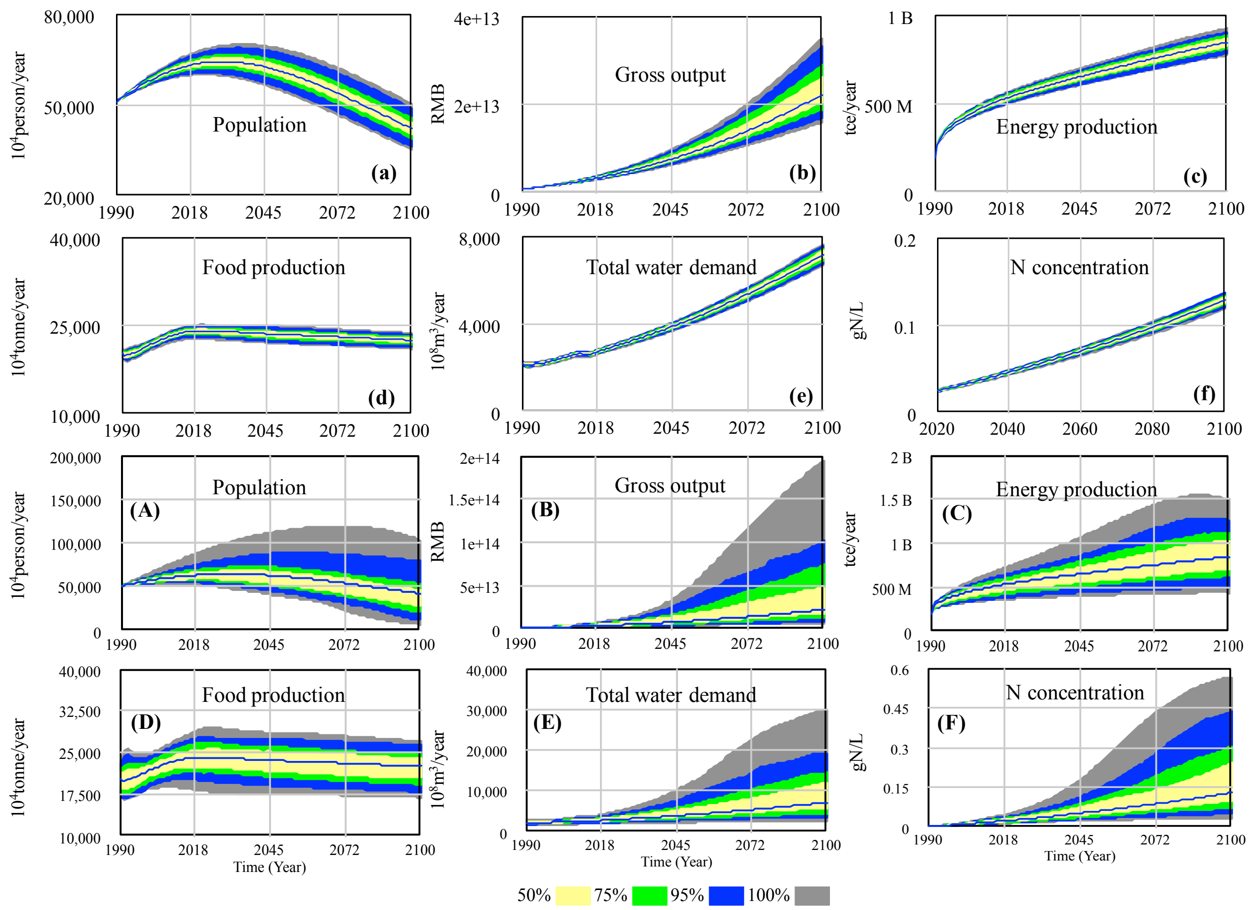

Figure 18. Sensitivity of the selected state variables

5.2 Model application

To test the capabilities of ANEMI_Yangtze, this section focuses on the applications of the model system for the baseline S_base scenario and S_energy scenario. S_base scenario assumes all parameters remain at their 2015 values during the simulation. S_energy scenario assumes the *energy share* of coal decreases linearly from around 60% (the 2015 share) to 30%, and the share of renewable energy (hydropower, nuclear, and new energy sources) increases from 15% to 30% by 2100. The simulation results are shown in Figures 19-20.

As the share of gas and renewable energy sources increases in S_energy scenario, the demand for those energy sources grows, placing more pressure on their production. *Energy production pressure effect* acts as a positive factor on *energy capital investment*. Therefore more money is poured into producing energy from gas and renewables sources. As more *energy capital* is mobilized for gas and renewable energy development, the improvement in *energy technology* advances correspondingly, leading to a decrease in *energy consumption intensity per unit GDP*, thus lowering the *energy demand* compared to the base run (Figure 19(a)). Besides, the combined effects of growing *energy capital investment* and *energy technology* advancement lead to a substantial increase in effective production effort, resulting in increases in gas and renewable energy productions (Figures 19 (f-i)). The production of coal is expected to decrease compared to the base run, along with its decrease in energy share (Figure 19(d)). Oil production remains at the base run level as its share remains the same value as in S_base scenario (Figure 19(e)). Those combined effects of the increase in gas and renewable energy productions and decrease in coal production result in a slight increase in the total production of energy compared to the base run result (Figure 19(b)).

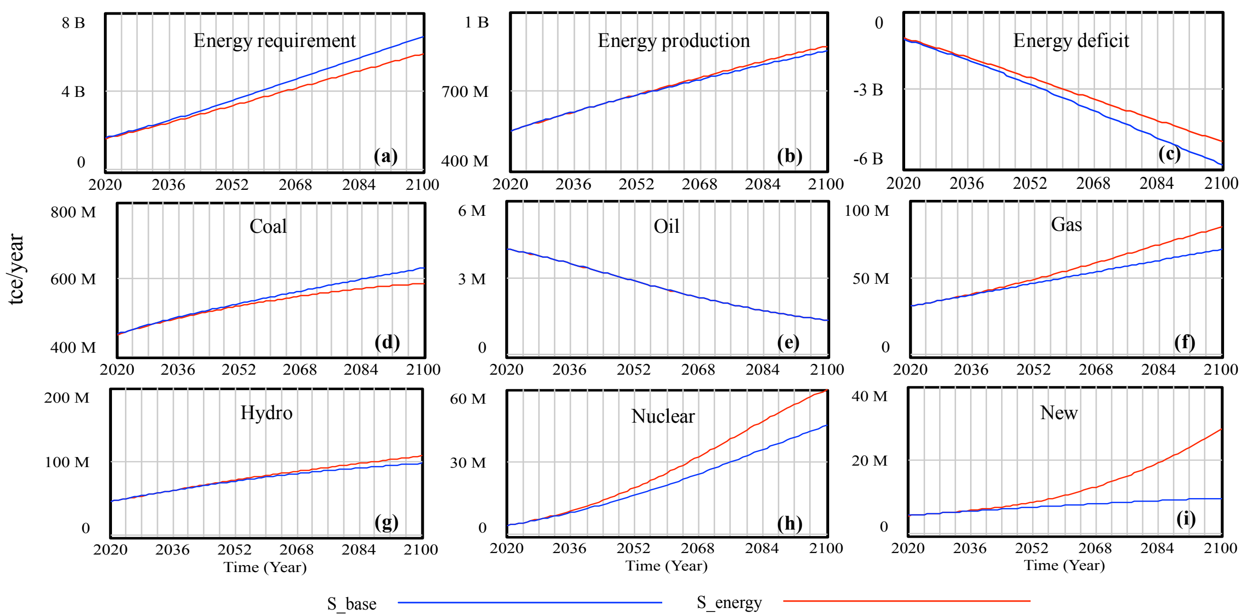

Figure 19. Effects of energy policy on energy system

The changing patterns of *energy consumption* have significant impacts on water and carbon systems. In S_base run, coal-fired thermal power plants dominate the *water demand* in industrial sector (approaches 600 billion m^3), whereas in S_energy scenario, industrial water demand drops considerably below 300 billion by the end of simulation as coal's share decreases from 60% to 30% (Figure 20(a)). Industrial sector replaces the agricultural sector and becomes the biggest water consumer after 2030. Under all definitions, *water stress* declines substantially, with all values lying below the critical value of 1 (Figures 20(b-e)). A decrease in industrial water demand and withdrawal also reduces industrial wastewater in accordance and lowers the level of nutrient concentration. The concentration level of nitrogen is shown in Figure 20(g); the results of phosphorus concentration, which share the same behaviour as the nitrogen, are not shown in the figure. By the end of the simulation, the carbon emissions fall from 4,800 Tg in the S_base run to about 2,500 Tg in S_energy scenario as a result of cutting the coal consumption by half.

The changing energy consumption pattern also impacts population growth and economic development to some degree. A slight increase in population is observed under S_energy scenario (Figure 20(h)) when compared to the base run. This is due to the reduction of nitrogen and phosphorus concentration levels, which improve *life expectancy* trough a variable - *lifetime multiplier from pollution*. As for the economy, even though there is a slightly higher supply of *labour force* resulting from an increase in population, the Belt's *gross output* in S_energy scenario is a little bit lower than in S_base output (Figure 20(i)). This is due to the reduced *energy requirement* as seen in Figure 20(a) and discussed in previous section. A decrease in *energy requirement* decreases the *capital-energy aggregate*, which then decreases the *operating capital*, leading to the decline in economic output. In this application, the effect of decreasing *operating capital* on economic output outpaces the effect of boosting the *labour force* on economic output.

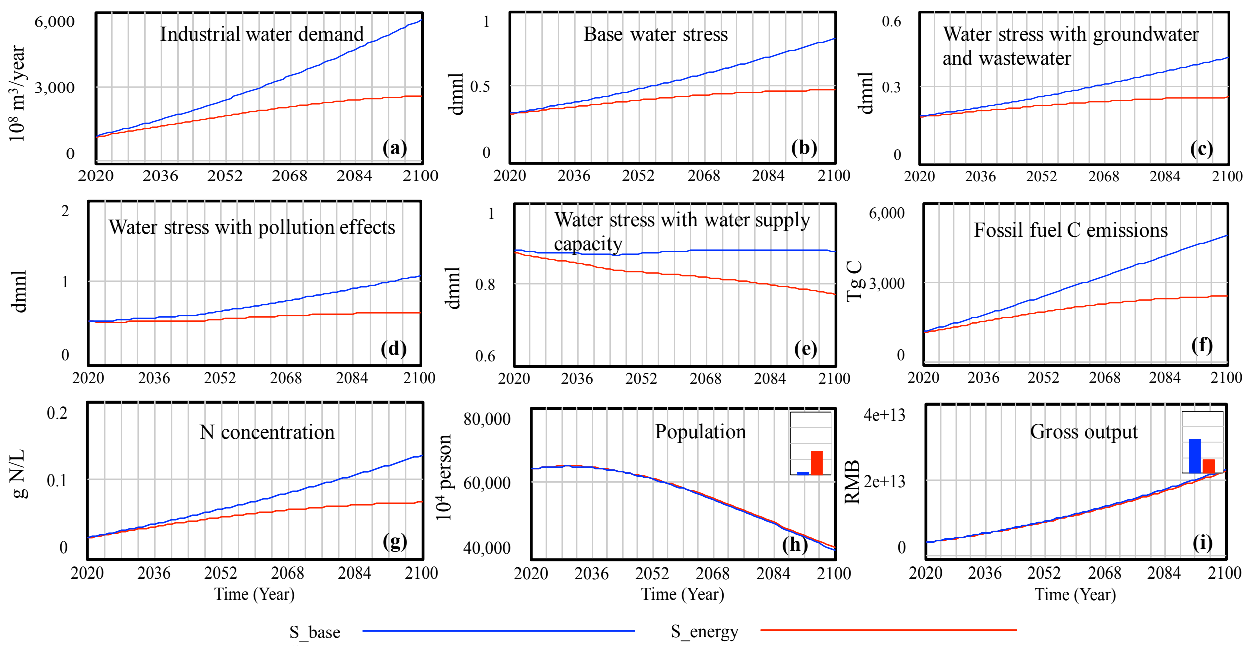

Figure 20. Effects of energy policy on the Belt system

6. Conclusion and discussion

To address the specific challenges facing Yangtze Economic Belt's sustainable development, ANEMI_Yangtze, which consists of the *Population*, *Economy*, *Land*, *Food*, *Energy*, *Water*, *Carbon*, *Nutrients*, and *Fish Sectors* was developed based on the feedback-based integrated global assessment model ANEMI3. This paper focuses on: (i) the identification of the cross-sectoral interactions and feedbacks involved in shaping the Belt's system behaviour over time; (ii) the identification of the feedbacks within each sector that drive the state variables in that sector; and (iii) the description of a new *Fish Sector* and modifications in the *Population*, *Food*, *Energy*, and *Water Sectors*, including the underlying theoretical basis for model equations. The model was validated by comparing simulated results with historical data. Sensitivity analysis was conducted by varying the parameters with high degree of uncertainty by -10% ~ +10% (mild variation scenario) and -50% ~ +50% (extreme variation scenario). Results demonstrate the model's robustness in modeling system behavioural.

In the application section, the impacts of shifting energy consumption patterns was investigated. As the Belt gradually shifts its *energy consumption* from coal to natural gas and renewable energy sources, the total *energy production* increases slightly. In contrast, the total *aggregated energy requirement* declines significantly due to the effects of e*nergy technology* advances. It is also found that the industrial *water demand* and the fossil fuel carbon emissions are greatly reduced, leading to a decrease in nutrient concentration levels and an increase in population. The Belt's *gross output* in S_energy scenario is lower than the base output as the effect of decreasing *operating capital*, which is caused by a decrease in total *aggregated energy requirement*, outpaces the effect of boosting the *labour force*. These findings enhance our integrated understanding of the dynamic behaviour of socio-economic development, natural resources depletion, and environmental impacts in the Belt. More in-depth model simulation analyses are needed to better understand the influences, responses, and feedbacks generic dynamic behavior of the Belt. The development of policy scenarios and the analyses of associated outcomes are presented in another paper (Jiang et al., 2021).

This paper focuses on presenting the feedback that drive the Belt's dynamic system behaviour based on the authors' current knowledge and understanding. It should, however, be kept in mind that some of the feedbacks might be missing due to the data necessary to describe these feedbacks are currently not available. For example, in China, fish plays an important dietary role and therefore, there should exist feedback connecting the *fish yield* and *food production*. Persistent pollution, a clear consequence of China's rapid economic development, should also be included. There are thus constant drivers to extend and improve the model framework as more data becomes available or as the state-of-the-knowledge progresses, or as scientific questions become more complex.

Code availability. The version of ANEMI_Yangtze described in this paper is archived on Zenodo (http://doi.org/10.5281/zenodo.4764138). The code can be opened using the Vensim software to view the model structure. A free Vensim PLE licence can be obtained from https://vensim.com, which can be used to view the stock and flow diagram that makes up the model structure. Due to the advanced features used in the ANEMI_Yangtze model, a Vensim DSS license is required to run the model.

Author contribution. **Haiyan Jiang**: Methodology, Investigation, Validation, Writing - original draft. **Slobodan P. Simonovic**: Conceptualization, Software, Writing - review & editing, Supervision. **Zhongbo Yu**: Funding acquisition, Writing - review & editing.

Competing interests. The authors declare that they have no conflict of interest.

Acknowledgements. This work was supported by the Belt and Road Special Foundation of the State Key Laboratory of Hydrology-Water Resources and Hydraulic Engineering (Grant No. 2020490111); the Fundamental Research Funds for the Central Universities (Grant No. B200202035); the National Key R&D Program of China (Grant No. 2016YFC0402710); National Natural Science Foundation of China (Grant No. 51539003, 41761134090, 51709074); the Special Fund of State Key Laboratory of Hydrology-Water Resources and Hydraulic Engineering (Grant No. 20195025612, 20195018812, 520004412). The authors are thankful for the financial support of the presented research provided to the second author by the Natural Sciences Research Council of Canada under the discovery grant program.

References

Akhtar, M. K., Simonovic, S. P., Wibe, J., and et al.: Future realities of climate change impacts: An integrated assessment study of Canada, Int. J. Global Warm., 17, 59-88, https://doi.org/10.1504/IJGW.2019.10017598, 2019.

Akhtar, M. K., Wibe, J., Simonovic, S. P., and et al.: Integrated assessment model of society-biosphere-climate-economy-energy system, Environ. Modell. Softw., 49, 1-21. http://doi.org/10.1016/j.envsoft.2013.07.006, 2013.

Allen, C., Metternicht, G., and Wiedmann, T.: National pathways to the Sustainable Development Goals (SDGs): A comparative review of scenario modelling tools, Environ. Sci. Policy, 66, 199-207, https://doi.org/10.1016/j.envsci.2016.09.008, 2016.

Bauer, N., Baumstark, L., and Leimbach, M.: The REMIND-R model: The role of renewables in the low-carbon transformation - first-best vs. second-best worlds, Climatic Change, 114, 145-168, https://doi.org/10.1007/s10584-011-0129-2, 2012.

Bazilian, M., Rogner, H., Howells, M., and et al.: Considering the energy, water and food nexus: Towards an integrated modelling approach, Energ. Policy, 39, 7896-7906, https://doi.org/10.1016/j.enpol.2011.09.039, 2011.

Breach, P.: Water Supply Capacity Development in the Context of Global Change, Electronic Thesis and Dissertation Repository, 6930. https://ir.lib.uwo.ca/etd/6930, 2020.

Breach, P. A., and Simonovic, S. P.: ANEMI: A tool for global change analysis, Plos One, 16, 0251489, https://doi.org/10.1371/journal.pone.0251489, 2021.

Calvin K., and Bond-Lamberty, B.: Integrated human-earth system modeling - state of the science and future directions, Environ. Res. Lett., 13, 063006, https://doi.org/10.1088/1748-9326/aac642, 2018.

Calvin, K., Patel, P., Clarke, L., and et al.: GCAM v5.1: Representing the linkages between energy, water, land, climate, and economic systems, Geosci. Model Dev., 12, 677-698, https://doi.org/10.5194/gmd-12-677-2019, 2019.

Cao, L., Zhang, Y., and Shi, Y.: Climate change effect on hydrological processes over the Yangtze River basin, Quatern. Int., 244, 202-210, https://doi.org/10.1016/j.quaint.2011.01.004, 2011.

Chen, D., Xiong, F., Wang, K., and et al.: Status of research on Yangtze fish biology and fisheries, Environ. Biol. Fish., 85, 337-357, https://doi.org/10.1007/s10641-009-9517-0, 2009.

Clark, W. A. V., Yi, D., and Zhang, X.: Do house prices affect fertility behavior in China? An empirical examination, Int. Regional Sci. Rev., 43(5), 423-449, https://doi.org/10.1177/0160017620922885, 2020.

Clayton, T., and Radcliffe, N.: Sustainability: A systems approach, Routledge, 2018.

Davies, E. G. R, and Simonovic, S. P.: ANEMI: A new model for integrated assessment of global change, Interdisciplinary Environmental Review, 11, 127-161, https://doi.org/10.1504/IER.2010.037903, 2010.

Davies, E. G. R, and Simonovic, S. P.: Global water resources modeling with an integrated model of the social-economic-environmental system, Adv. Water Resour., 34, 684-700, https://doi.org/10.1016/j.advwatres.2011.02.010, 2011.

Department of Energy at National Bureau of Statistics (DENBS): China Energy Statistical Yearbook in 2015. China Statistics Press, Beijing, 2016 (in Chinese).

Dermody, B. J., Sivapalan, M., Stehfest, E., and et al.: A framework for modelling the complexities of food and water security under globalisation, Earth Syst. Dynam., 9, 103-118, https://doi.org/10.5194/esd-2017-38, 2018.

Dettling, L. J., Kearney, M. S.: House prices and birth rates: The impact of the real estate market on the decision to have a baby, J. Public Econ., (1), 82-100, https://doi.org/10.1016/j.jpubeco.2013.09.009, 2014.

Dinar, A., Tieu, A., and Huynh, H.: Water scarcity impacts on global food production, Glob. Food Secur., 23(3), 212-226, https://doi.org/10.1016/j.gfs.2019.07.007, 2019.

D'Odorico, P., Davis, K. F., Rosa, L., and et al.: The global food-energy-water nexus, Rev. Geophys., 56, 456-531, https://doi.org/10.1029/2017RG000591, 2018.

European Commission: Energy in Europe, European energy to 2020: A scenario approach. Belgium: Directorate general for energy, 1996.

Fang, Y., Zhang, W., Cao, J., and et al.: Analysis on the current situation and development trend of energy resources in China, Conservation and Utilization of Mineral Resources, 4, 34-42, 2018, (in Chinese).

Fiddaman, T. S.: Feedback complexity in integrated climate-economy models, Department of Operations Management and System Dynamics, Massachusetts Institute of Technology, Cambridge, Massachusetts, 1997.

Fisher-Vanden, K., and Weyant, J.: The evolution of integrated assessment: Developing the next generation of use-inspired integrated assessment tools, Annu. Review Resour. Econ., 12, 471-487, https://doi-org/10.1146/annurev-resource-110119-030314, 2020.

Forrester, J. W.: Industrial dynamics. Cambridge, MA: Massachusetts Institute of Technology Press, 1961.

Fu, B.: Promoting geography for sustainability, Geography and Sustainability, 1(1), 1-7, https://doi.org/10.1016/j.geosus.2020.02.003, 2020.

Giorgi, F., Im, E. S., Coppola, E., and et al.: Higher hydroclimatic intensity with global warming, J.Climate, 24(20), 5309-5324, https://doi.org/10.1175/2011JCLI3979.1, 2011.

Gilbert, D. J., McKenzie, J. R., Davies, N. M., and et al.: Assessment of the SNA 1 stocks for the 1999-2000 fishing year. New Zealand Fisheries Assessment Report, 38, 52, 2000.

Goudriaan, J., and Ketner, P.: A simulation study for the global carbon cycle, including man's impact on the biosphere, Climatic Change, 6(2), 167-192, 1984.

Gu, H., Yu, Z., Wang, G., and et al.: Impact of climate change on hydrological extremes in the Yangtze river basin, China, Stoch. Env. Res. Risk A., 29, 693-707, https://doi.org/10.1007/s00477-014-0957-5, 2015.

Henze. M., and Comeau, Y.: Wastewater Characterization. In: Biological Wastewater Treatment: Principles Modelling and Design. IWA Publishing, London, UK, 33-52, 2008.

Hertwich, E. G., Gibon, T., Bouman, E. A., and et al.: Integrated life-cycle assessment of electricity-supply scenarios confirms global environmental benefit of low-carbon technologies, P. Natl. Acad. Sci. USA, 112, 6277-6282, https://doi.org/10.1073/pnas.1312753111, 2015.

Holman, I. P., Rounsevell, M. D. A., Cojacaru, G., and et al.: The concepts and development of a participatory regional integrated assessment tool, Climatic Change, 90, 5-30, https://doi.org/10.1007/s10584-008-9453-6, 2008.

Hopwood, B., Mellor, M., and O'Brien, G.: Sustainable development: Mapping different approaches, Sustainable Development, 13, 38-52, https://doi.org/10.1002/sd.244, 2005.

Hui, E., Xian, Z., and Jiang, H:. Housing price, elderly dependency and fertility behaviour, Habitat Int., 36(2), 304-311, https://doi.org/10.1016/j.habitatint.2011.10.006, 2012.

Jeon, S., Roh, M., Oh, J., and et al.: Development of an integrated assessment model at provincial level: GCAM-Korea, Energies, 13, 2565, https://doi.org/10.3390/en13102565, 2020.

Jia, B., Zhou, J., Zhang, Y., and et al.: System dynamics model for the coevolution of coupled water supply - power generation - environment systems : Upper Yangtze river Basin , China, J. Hydrol., 593, 125892, https://doi.org/10.1016/j.jhydrol.2020.125892, 2021.

Jiang, H., and Simonovic, S. P.: ANEMI_Yangtze - A regional integrated assessment model for the Yangtze Economic Belt in China. Water Resources Research Report no. 110, Facility for Intelligent Decision Support, Department of Civil and Environmental

Engineering, London, Ontario, Canada, 75 pages. ISBN: (print) 978-0-7714-3155-5; (online) 978-0-7714-3156-2, 2021. https://www.eng.uwo.ca/research/iclr/fids/publications/products/111.pdf.

Jiang, H., Simonovic, S. P., Yu, Z., and et al.: System dynamics simulation model for flood management of the three gorges reservoir, J. Water Res. Plan. Man., 146, 05020009, https://doi.org/10.1061/(ASCE)WR.1943-5452.0001216, 2020.

Jiang, H., Simonovic, S. P., Yu, Z., and et al.: What are the main challenges facing the sustainable development of China's Yangtze Economic Belt in the future? An integrated view, Environ. Res. Commun., 3, 115005, https://doi.org/10.1088/2515-7620/ac35bd, 2021.

Ju, H., Liu, Q., Li, Y., and et al.: Multi-stakeholder efforts to adapt to climate change in China's agricultural sector, Sustainability, 12, https://doi.org/10.3390/su12198076, 2020.

Klein, J. T., Grossenbacher-Mansuy, W., Häberli, R., and et al.: Transdisciplinarity: Joint problem solving among science, technology, and society: An effective way for managing complexity, Springer Science & Business Media, 2001.

Kong, L., Zheng, H., Rao, E., and et al.: Evaluating indirect and direct effects of eco-restoration policy on soil conservation service in Yangtze River Basin, Sci. Total Environ., 631, 887-894, https://doi.org/10.1016/j.scitotenv.2018.03.117, 2018.

Kriegler, E., Bauer, N., Popp, A., and et al.: Fossil-fueled development (SSP5): An energy and resource intensive scenario for the 21st century, Global Environ. Chang., 42, 297-315, https://doi.org/10.1016/j.gloenvcha.2016.05.015, 2017.

Lee, E. S.: A Theory of Migration. Demography, 3(1), 47-57, 1966.

Lei, G., Fu, C., Zhang, L., and et al.: The changes in population floating and their influencing factors in China based on the sixth census, Northwest Population Journal, 34(05), 1-8, https://doi.org/10.15884/j.cnki.issn.1007-0672.2013.05.017, 2013. (in Chinese)

Li, Y., Acharya, K., and Yu, Z.: Modeling impacts of Yangtze River water transfer on water ages in Lake Taihu, China, Ecol. Eng., 37, 325-334, https://doi.org/10.1016/j.ecoleng.2010.11.024, 2011.

Li, Z., He, Y., Pu, T., and et al.: Changes of climate, glaciers and runoff in China's monsoonal temperate glacier region during the last several decades, Quatern. Int., 218, 13-28, https://doi.org/10.1016/j.quaint.2009.05.010, 2010.

Liu, L., and Ding, Y.: Hydraulic resources and hydropower planning in the Yangtze River Basin, Yangtze River, 44, 69-71, 2013, (in Chinese).

Liu, J. G., Dietz, T., Carpenter, S. R., and et al.: Complexity of coupled human and natural systems, Science, 317 (5844), 1513-1516, https://doi.org/10.1126/science.1144004, 2007.

Loulou, R.: ETSAP-TIAM: The TIMES integrated assessment model. Part II: Mathematical formulation, Comput. Manag. Sci., 5, 41-66, https://doi.org/10.1007/s10287-007-0045-0, 2007.

Ma, L., and Yu, Z.: Influencing factors of Chinese average life expectancy, Economic Research Guide, (01), 161-162, 2009.

Mackenzie, F. T., Ver, L. M., Sabine, C., and et al.: C, N, P, S global biogeochemical cycles and modeling of global change, Interactions of C, N, P and S Biogeochemical Cycles and Global Change, Springer, Verlag, 1-61, 1993.

Matsuoka, Y., Kainuma, M., and Morita, T.: Scenario analysis of global warming using the Asian-Pacific integrated model (AIM), Energ. Policy, 23, 357-371, 10.1016/0301-4215(95), 90160-9, 1995.

Meadows, D. L., Behrens, W.W., Meadows, D. H., and et al.: Dynamics of Growth in a Finite World. Wright-Allen Press, Inc. Cambrigde, Massachusetts, 1974.

Messner, S., and Strubegger, M.: User's Guide for MESSAGE III, Working Paper WP-95-069, International Institute for Applied Systems Analysis (IIASA), Laxenburg, Austria, 1995, p. 164.

Messner, S., and Schrattenholzer, L.: MESSAGE-MACRO: linking an energy supply model with a macroeconomic module and solving it iteratively, Energy, 25, 267-282, https://doi.org/10.1016/S0360-5442(99)00063-8, 2000.

MIIT: Innovation-driven industrial transformation and upgrading plan for the Yangtze River Economic Belt. Ministry of Industry and Information Technology of the People's Republic of China, 2016.

National Development and Reform Commission (NDRC): Development and planning outline of the Yangtze River Economic Belt officially released, 2016. http://www.sc.gov.cn/10462/10758/10760/10765/2016/9/20/10396398.shtml

Niva, V., Cai, J., Taka, M., and et al.: China's sustainable water-energy-food nexus by 2030: Impacts of urbanization on sectoral water demand, J. Clean. Prod., 251, 119755, https://doi.org/10.1016/j.jclepro.2019.119755, 2020.

Nordhaus, W. D., and Boyer, J.: Warming the world: Economic models of global warming. The MIT Press, Cambridge, Massachusetts, U.S.A., 2000.

Pautrel, X.: Pollution and life expectancy: How environmental policy can promote growth, Ecol. Econ., 68(4), 1040-1051, https://doi.org/10.1016/j.ecolecon.2008.07.011, 2009.

Pedercini, M., Arquitt, S., Collste, D., and et al.: Harvesting synergy from sustainable development goal interactions, P. Natl. Acad. Sci. USA, 46, 23021-23028, https://doi.org/10.1073/pnas.1817276116, 2019.

Qin, B. Q., Wang, X. D., Tang, X. M., and et al.: Drinking water crisis caused by eutrophication and cyanobacterial bloom in Lake Taihu: cause and measurement, Advances in Earth Science, 22, 896-906, https://doi.org/10.3321/j.issn:1001-8166.2007.09.003, 2007. (in Chinese)

Qu, W., Barney, G., Symalla, D., and et al.: Threshold 21: National sustainable development model, Integrated Global Models of Sustainable Development, 2, 78-87, 1995.

Qu, W., Shi, W., Zhang, J., and et al.: T21 China 2050: A tool for national sustainable development planning, Geography and Sustainability, 1(1), 33-46, https://doi.org/10.1016/j.geosus.2020.03.004, 2020.

Shen, J.: Increasing internal migration in China from 1985 to 2005: Institutional versus economic drivers, Habitat Int., 39, 1-7, https://doi.org/10.1016/j.habitatint.2012.10.004, 2013.

Shi, W., Ou, Y., Smith, S. J., and et al.: Projecting state-level air pollutant emissions using an integrated assessment model: GCAM-USA, Appl. Energ., 208, 511-521, https://doi.org/10.1016/j.apenergy.2017.09.122, 2017.

Shiklomanov, I. A.: Appraisal and assessment of world water resources, Water Int., 25, 11-32, https://doi.org/10.1080/02508060008686794, 2000.

Simonovic, S. P.: Global water dynamics: Issues for the 21st century, Journal of Water Science and Technology, 45, 53-64, https://doi.org/10.2166/wst.2002.0143, 2002.

Simonovic, S. P.: Managing water resources: Methods and tools for a systems approach. London: Earthscan James & James, 2009.

Simonovic, S. P.: World water dynamics: Global modeling of water resources, J. Environ. Manage., 66, 249-267, https://doi.org/10.1006/jema.2002.0585, 2002a.

Song, Q.: Study on the wind resource distribution and wind power planning in China, North China Electric Power University, 2013, (in Chinese).

State Grid Energy Research Institution (SGERI), and China Nuclear Power Development Center (CNPD): Research on nuclear power development planning in China. China Atomic Energy Press, 2019, (in Chinese).

Stehfest, E., van Vuuren, D., Kram, T., and et al.: Integrated assessment of global environmental change with IMAGE 3.0: Model description and policy applications, PBL Netherlands Environmental Assessment Agency, ISBN: 978-94-91506-71-0, 2014.

Su, B., Huang, J., Zeng, X., and et al.: Impacts of climate change on streamflow in the upper Yangtze River basin, Climatic change, 141, 533-546, https://doi.org/10.1007/s10584-016-1852-5, 2017.

Su, M.: Research on the coordinated development of energy in the Yangtze River Economic Zone, Macroeconomic Management, 12, 37-41, 2019 (in Chinese).

Su, Y., Tesfazion, P., and Zhao, Z.: Where are the migrants from? Inter- vs. intra-provincial rural-urban migration in China, China Economic Review, 47, 142-155, https://doi.org/10.1016/j.chieco.2017.09.004, 2018.

Sullivan, P., Krey, V., and Riahi, K.: Impacts of considering electric sector variability and reliability in the MESSAGE model, Energy Strateg. Rev., 1, 157-163, https://doi.org/10.1016/j.esr.2013.01.001, 2013.

van Beek, L., Hajer, M., Pelzer, P., and et al.: Anticipating futures through models: the rise of Integrated Assessment Modelling in the climate science-policy interface since 1970, Global Environ. Chang., 65, 102191, https://doi.org/10.1016/j.gloenvcha.2020.102191, 2020.

van Vuuren, D. P., Kok, M., Lucas, P. L., and et al.: Pathways to achieve a set of ambitious global sustainability objectives by 2050: Explorations using the IMAGE integrated assessment model, Technol. Forecast. Soc., 98, 303-323, https://doi.org/10.1016/j.techfore.2015.03.005, 2015.

Wang, H: Yangtze Yearbook, Changjiang Water Resources Commission of Ministry of Water Resources, 2015, (in Chinese).

Wang, H., Liu, L., Yang, F., and et al.: System dynamics modeling of China's grain forecasting and policy simulation, Journal of System Simulation, 21, 3079-3083, 2009. (in Chinese)

Wang, Z., Nguyen, T., and Westerhoff, P.: Food-energy-water analysis at spatial scales for districts in the Yangtze river basin (China), Environ. Eng. Sci., 36, 789-797, https://doi.org/10.1089/ees.2018.0456, 2019.

Xie, H., and Wang, B.: An empirical analysis of the impact of agricultural product price fluctuations on China's grain yield, Sustainability, 9, 906, https://doi.org/10.3390/su9060906, 2017.

Xu, X., Yang, G., Tan, Y., and et al.: Ecosystem services trade-offs and determinants in China's Yangtze River Economic Belt from 2000 to 2015, Sci. Total Environ., 634, 1601-1614, https://doi.org/10.1016/j.scitotenv.2018.04.046, 2018.

Yao, G., Gao, Z., and Li, X.: Evaluation of coal resources bearing capacity in China, China Mining Magazine, 29, 1-7, 2020 (in Chinese).

Yangtze River Water Resources Commission (YRWRC): Water resources bulletin of the Yangtze river basin and the southwest rivers in China 2015. Yangtze River Press, Wuhan, 2016 (in Chinese).

Ye, L., Wei, X., Li, Z., and et al.: Climate change impact on China food security in 2050, Agron. Sustain. Dev., 33, 363-374, https://doi.org/10.1007/s13593-012-0102-0, 2013.

Yi, B. L., Yu, Z. T., and Liang, Z. S.: Gezhouba Water Control Project and four famous fishes in the Yangtze River, Wuhan: Hubei Science and Technology Press, 1988, (in Chinese with English abstract).

Yu, S., Yarlagadda, B., Siegel, J. E., and et al.: The role of nuclear in China's energy future: Insights from integrated assessment, Energ. Policy, 139, 111344, https://doi.org/10.1016/j.enpol.2020.111344, 2020.

Yu, Z., Gu, H., Wang, J., and et al.: Effect of projected climate change on the hydrological regime of the Yangtze River Basin, China, Stoch. Env. Res. Risk A., 32, 1-16, https://doi.org/10.1007/s00477-017-1391-2, 2018.

Zeng, Y., and Hesketh, T.: The effects of China's universal two-child policy, The Lancet, 388, 1930-1938, https://doi.org/10.1016/S0140-6736(16)31405-2, 2016.

Zhang, C., Zhong, L., Fu, X., and et al.: Revealing water stress by the thermal power industry in China based on a high spatial resolution water withdrawal and consumption inventory, Environ. Sci. Technol., 50, 1642-1652, https://doi.org/10.1021/acs.est.5b05374, 2016.

Zhang, H., Kang, M., Shen, L., and et al.: Rapid change in Yangtze fisheries and its implications for global freshwater ecosystem management, Fish Fish., 21, 601-620, https://doi.org/10.1111/faf.12449, 2020.

Zhang, H., Li, J. Y., Wu, J. M., and et al.: Ecological effects of the first dam on Yangtze main stream and future conservation recommendations: A review of the past 60 years, Appl. Ecol. Env. Res., 15, 2081-2097, https://doi.org/10.15666/aeer/1504_20812097, 2017.

Zhao, F., and Fan, Z.: The inhibitory effect of high housing prices on population inflows in the megacities: Based on the empirical evidence from the four cities of Beijing, Shanghai, Guangzhou and Shenzhen, Urban Studies, 26(03), 41-48, 2019. (in Chinese)

Zhu, R., Ma, S., Yang, Z., and et al.: Atlas of solar energy resources by province in China. Beijing: China Meteorological Administration, 2006, (in Chinese).